

# Accepted Manuscript

(3Z)-3-(2-[4-(Aryl)-1,3-thiazol-2-yl]hydrazin-1-ylidene)-2,3-dihydro-1*H*-indol-2-one Derivatives as Dual Inhibitors of HIV-1 Reverse Transcriptase

Rita Meleddu, Simona Distinto, Angela Corona, Giulia Bianco, Valeria Cannas, Francesca Esposito, Anna Artese, Stefano Alcaro, Peter Matyus, Dora Bogdand, Filippo Cottiglia, Enzo Tramontano, Elias Maccioni

PII: S0223-5234(15)00128-2

DOI: [10.1016/j.ejmech.2015.02.032](https://doi.org/10.1016/j.ejmech.2015.02.032)

Reference: EJMECH 7714

To appear in: *European Journal of Medicinal Chemistry*

Received Date: 3 September 2014

Revised Date: 13 January 2015

Accepted Date: 19 February 2015

Please cite this article as: R. Meleddu, S. Distinto, A. Corona, G. Bianco, V. Cannas, F. Esposito, A. Artese, S. Alcaro, P. Matyus, D. Bogdand, F. Cottiglia, E. Tramontano, E. Maccioni, (3Z)-3-(2-[4-(Aryl)-1,3-thiazol-2-yl]hydrazin-1-ylidene)-2,3-dihydro-1*H*-indol-2-one Derivatives as Dual Inhibitors of HIV-1 Reverse Transcriptase, *European Journal of Medicinal Chemistry* (2015), doi: 10.1016/j.ejmech.2015.02.032.

This is a PDF file of an unedited manuscript that has been accepted for publication. As a service to our customers we are providing this early version of the manuscript. The manuscript will undergo copyediting, typesetting, and review of the resulting proof before it is published in its final form. Please note that during the production process errors may be discovered which could affect the content, and all legal disclaimers that apply to the journal pertain.

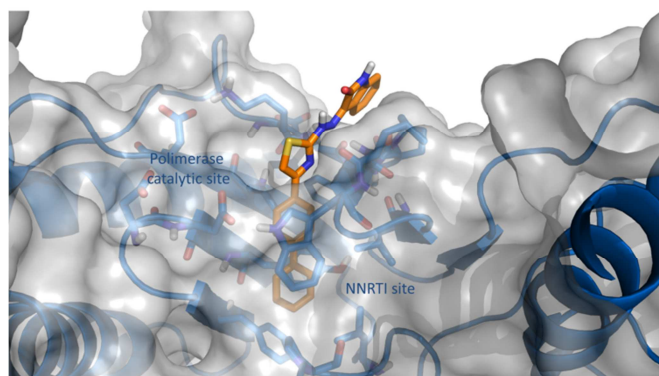


**Graphical abstract**

(3Z)-3-(2-[4-(Aryl)-1,3-thiazol-2-yl]hydrazin-1-ylidene)-2,3-dihydro-1H-indol-2-one Derivatives as Dual Inhibitors of HIV-1 Reverse Transcriptase

*Rita Meleddu, Simona Distinto, Angela Corona, Giulia Bianco, Valeria Cannas, Francesca Esposito, Anna Artese, Stefano Alcaro, Peter Matyus, Dora Bogdand, Filippo Cottiglia, Enzo Tramontano, Elias Maccioni.*

The synthesis of indolinone derivatives based on a previously identified analogue led to the confirmation of this scaffold as a promising hit for the design of dual inhibitors of the two reverse transcriptase associated functions, DNA polymerase and ribonuclease H (RNase H) activities.



**Title**

(3Z)-3-(2-[4-(Aryl)-1,3-thiazol-2-yl]hydrazin-1-ylidene)-2,3-dihydro-1*H*-indol-2-one Derivatives as Dual Inhibitors of HIV-1 Reverse Transcriptase

**Authors**

Rita Meleddu<sup>a</sup>, Simona Distinto<sup>a</sup>, Angela Corona<sup>b</sup>, Giulia Bianco<sup>a</sup>, Valeria Cannas<sup>a</sup>, Francesca Esposito<sup>b</sup>, Anna Artese<sup>c</sup>, Stefano Alcaro<sup>c</sup>, Peter Matyus<sup>d</sup>, Dora Bogdand<sup>d</sup>, Filippo Cottiglia<sup>a</sup>, Enzo Tramontano<sup>b</sup>, Elias Maccioni<sup>a\*</sup>.

**Affiliations**

<sup>a</sup>Department of Life and Environmental Sciences, University of Cagliari, Via Ospedale 72, 09124 Cagliari, Italy

<sup>b</sup>Department of Life and Environmental Sciences, University of Cagliari, Cittadella Universitaria di Monserrato, SS554, 09042 Monserrato, Cagliari, Italy

<sup>c</sup>Dipartimento di Scienze della Salute, Università Magna Graecia di Catanzaro, Campus "S. Venuta", Viale Europa, 88100 Catanzaro, Italy

<sup>d</sup>Department of Organic Chemistry, Högies Endre utca 7, 1092, Semmelweis University, Budapest, Hungary

\*To whom correspondence should be addressed. S.D, Department of Life and Environmental Sciences, University of Cagliari, Via Ospedale 72, 09124 Cagliari, Italy; Tel: +39 0706758550; Fax +39 0706758553, E-mail: maccione@unica.it.

## Abstract

The HIV-1 Reverse Transcriptase (RT) is a validated and deeply explored biological target for the treatment of AIDS. However, only drugs targeting the RT-associated DNA polymerase (DP) function have been approved for clinical use. We designed and synthesised a new generation of HIV-1 RT inhibitors, based on the (3Z)-3-(2-[4-(aryl)-1,3-thiazol-2-yl]hydrazin-1-ylidene)-2,3-dihydro-*IH*-indol-2-one scaffold. These compounds are active towards both RT-associated functions, DNA polymerase and ribonuclease H. The structure, biological activity and mode of action of the new derivatives have been investigated. In particular, the nature of the aromatic group in the position 4 of the thiazole ring plays a key role in the modulation of the activity towards the two RT-associated functions.

**Keywords:** Antiviral agents, HIV-1 RT dual inhibitors, HIV-1, molecular modelling, RNase H, (3Z)-3-(2-[4-(aryl)-1,3-thiazol-2-yl]hydrazin-1-ylidene)-2,3-dihydro-*IH*-indol-2-ones

## Abbreviations

HIV-1, Human Immunodeficiency Virus type 1; HAART, Highly Active Antiretroviral Therapy; RT, Reverse Transcriptase; RTIs, RT inhibitors; NRTIs/NtRTIs, Nucleoside/Nucleotide RTIs; NNRTI Non-Nucleoside RTIs; DP, DNA polymerase; RNase H, ribonuclease H; RHIs, RNase H inhibitors; NNRTIBP, NNRTIs binding pocket; PLK4, polo-like kinase 4; BACE1, Beta-secretase 1; CRTH2 (DP2), chemoattractant receptor-homologous molecule expressed on Th2 cells (D2 prostanoid receptor); NOE, Nuclear Overhauser Effect; NMR, Nuclear Magnetic Resonance; R.T., room temperature; RNase H, Ribonuclease H; MM-GBSA, the Molecular Mechanics Generalized Born/Surface Area; MMFFs, Merck Molecular Force Field; GB/SA, Generalized Born/Surface Area; PRCG, Polak-Ribier Coniugate Gradient; QPLD, Quantum Mechanic-Polarized ligand Docking.

## 1. Introduction

The current approved treatment for Human Immunodeficiency Virus type 1 (HIV-1) infection is based on the highly active antiretroviral therapy (HAART), that associates a combination of antiviral agents, targeting different steps of the virus replication cycle [1, 2]. This multidrug therapeutic regimen leads to the reduction of the amount of circulating virus, in some cases below the current blood testing techniques detectable level, and allows high control of the infection. Moreover, it leads to the reduction of drug resistance occurrence, decrease of mortality and morbidity rates, and an overall improvement of patients quality of life [3]. However, due to the chronic nature of HIV infection, a lifelong therapy is required and both adherence to treatment and the management of drug-related toxicities are issues to deal with.

Although numerous strategies of simplified treatment have been explored in order to further improve patient quality of life, while maintaining treatment success, RT inhibitors (RTIs), both Nucleoside/Nucleotide RTIs (NRTIs/NtRTIs) and Non-Nucleoside RTIs (NNRTIs) are always included in the HAART regimen [1, 2], due to the key role of RT in the early phase of the HIV-1 life cycle.

HIV-1 RT catalyses the reverse transcription process which consists of the conversion of a single strand viral RNA into a double strand viral DNA via the formation of a RNA-DNA hybrid. To perform this activity two main catalytic functions are associated in one enzyme, DNA polymerase (DP) and ribonuclease H (RNase H).

However, despite the fact that both functions are validated drug targets, since also RNase H function is essential for the reverse transcription process [4, 5], no inhibitor that target this enzymatic activity has been introduced in therapy until now [6, 7].

Most RNase H inhibitors (RHIs), designed and studied so far, act by chelating the  $Mg^{2+}$  ions within the active site [8-15]. However other mechanisms of action have been reported for hydrazone [16], naphthyridinone [17], anthraquinone [18] and propenone [19] derivatives.

The latter compounds are capable of binding an allosteric pocket close to the NNRTIs binding pocket (NNRTIBP) and of inhibiting the RNase H function by a long range allosteric effect.

We have recently reported the identification of a new scaffold for dual inhibition of both HIV-1 RT-associated RNase H and DP functions [20]. Among all the identified molecules, compound **1** (3Z)-3-(2-[4-(3,4-dihydroxyphenyl)-1,3-thiazol-2-yl]hydrazin-1-ylidene)-2,3-dihydro-1*H*-indol-2-one (Figure 1) resulted as the best performing derivative with IC<sub>50</sub> value in the low micromolar range [20].

Firstly, to gain insights into the drug novelty potential of compound **1**, we wanted to investigate its mode of action by measuring its capability to chelate Mg<sup>2+</sup> ions, since RNase H active site inhibitors have been reported to chelate the Mg<sup>2+</sup> [21]. Secondly, we examined if cross resistance with NNRTI resistant RTs could be observed for compound **1**, since this behaviour has been reported for those compounds that interact with the allosteric RNase H pocket, close to the NNRTIBP [16, 18, 22]. Results showed that compound **1** did not chelate Mg<sup>2+</sup> (Figure 2), but its activity was slightly affected when tested on the Lys103Asn and Tyr181Cys RTs, two NNRTI resistant mutant enzymes [20]. These results suggested that compound **1** could have a mode of action similar to previously reported hydrazone derivatives [16, 17]. Hence, we performed biochemical and docking experiments that, in agreement with the biochemical data, indicated compound **1** able to bind RT in the region indicated by Himmel et al in previous works [16, 17]. Therefore, in order to investigate the influence of structural modifications on the biological activity of compound **1**, we synthesised a small library of (3Z)-3-(2-[4-(aryl)-1,3-thiazol-2-yl]hydrazin-1-ylidene)-2,3-dihydro-1*H*-indol-2-ones.

As in the original compound **1**, we have conserved the indolinone and thiazole moieties that have been reported as important fragments in a number of bioactive molecules, such as selective chymase inhibitors [23], polo-like kinase 4 (PLK4) inhibitors [24], Beta-secretase 1 (BACE1) inhibitors [25], chemoattractant receptor-homologous molecule expressed on Th2 cells (D2 prostanoid receptor) (CRTH2 (DP2)) antagonists [26], MAO inhibitors [27] anti-mycobacterial [28,

29], anti-Candida [30], and antimicrobial [31]. In the present work, we introduced differently substituted phenyl moieties at the position 4 of the thiazole ring in place of the 3,4-dihydroxyphenyl group, and evaluated their ability to behave as dual RT-associated functions inhibitors (Figure 1).

**Figure 1 here**

## 2. Chemistry

(3*Z*)-3-(2-[4-(aryl)-1,3-thiazol-2-yl]hydrazin-1-ylidene)-2,3-dihydro-1*H*-indol-2-ones (**EMAC2072-2082**) were synthesized starting from 2,3-dihydro-1*H*-indole-2,3-dione. This was reacted with thiosemicarbazide in 2-propanol to give 2-oxo-2,3-dihydro-1*H*-indol-3-thiosemicarbazone. Equimolar amounts of semicarbazone synthesized and of the appropriate  $\alpha$ -halogeno-arylketone were then stirred in 2-propanol to give the desired final compounds, as depicted in Scheme 1.

**Scheme 1 here**

Compounds **EMAC2072-2082** were characterised by means of both analytical and spectroscopic methods. Their analytical and spectroscopic properties are reported in Table S1 and S2.

The possible formation of both *E* and *Z* diastereoisomers along the C=N double bond was investigated by Nuclear Overhauser Effect (NOE) experiments.

In each compound the irradiation of the indole CH-4 only changed the intensity of the neighbouring CH protons, whereas upon irradiation of the hydrazone NH signal, no intensity change was observed. This indicated that the two protons have no measurable NOEs since they are spatially too far from each other. This distance is in agreement with the “*Z*” configuration. Therefore, *Z*-configuration of each compound could be confirmed (Figure S1).

## 3. Results and discussion

Compounds **EMAC2072-2082**, were evaluated for their ability to inhibit both HIV-1 RT associated RNase H and DP functions (Table 1) using as reference controls compound **1**, **Efavirenz**

(EFV), and **RDS 1643** [13], a diketoacid inhibitor of the RNase H function that binds the catalytic site.

**Table1 here**

All tested compounds, with the exception of compound **EMAC2081**, exhibited dual inhibitory activity towards both HIV-1 RT functions, confirming that the (3Z)-3-(2-[4-(aryl)-1,3-thiazol-2-yl]hydrazin-1-ylidene)-2,3-dihydro-1*H*-indol-2-one scaffold could be considered a promising candidate for the design of HIV-1 RT dual functions inhibitor [20]. Interestingly, while compound **1** showed a specificity index (SpI), expressed as the ratio of the RNase H IC<sub>50</sub> value *versus* the DP IC<sub>50</sub> value, favourable to the DP function (SpI = 3,5), all new derivatives exhibited a SpI favourable to the RNase H function. These results suggest that the compounds activity and specificity on the two functions is strongly influenced by the presence and the nature of the substituents in the 4-phenylthiazole system.

In fact, in the case of compound **EMAC2081**, bearing the un-substituted 4-phenylthiazole moiety, almost no activity towards both functions was observed. Conversely, the introduction of a 4-(4-biphenyl)thiazole moiety (**EMAC2076**) led to one of the most potent compounds, with a SpI of 0.11. However, the introduction of a 4-(3-nitrophenyl)thiazole (**EMAC2078**) appears as the most performing substitution with respect to DP and RNase H inhibition. Instead, the introduction of the 2,4-difluorophenyl thiazole (**EMAC2077**) or the 4-(4-biphenyl)thiazole (**EMAC2076**) is effective towards the RNase H inhibition. Therefore, a mixture of steric and electronic effects should be blended in order to achieve the best activity towards the two RT associated functions. Moreover, the double substitution with halogen atoms in the positions 2 and 4 of the 4-phenyl thiazole is also effective with respect to the mono-substitution. Thus, compounds **EMAC2072** and **EMAC2073** are less potent than their di-substituted analogues **EMAC2082** and **EMAC2077**.

In this respect, fluorine demonstrated to be more efficient than chlorine, probably due to the higher capability to act as hydrogen bond acceptor. Indeed the size of fluorine is intermediate between that of hydrogen and oxygen and its van der Waals radius (1.47 Å) could be compared to

those of hydrogen (1.2 Å) and oxygen (1.57 Å). As a matter of fact, we have observed that small changes in structure have dramatic effects on activity.

Dual activity might originate from a set of ligand-enzyme interactions, such as the formation of complexes between the ligand and the NNRTIBP, the RNase H allosteric site, and the RNase H catalytic site. Therefore, a mode of action investigation by means of biochemical and computational methods was performed, in order to identify the mechanism of action and the most probable binding modes of these compounds.

Firstly, we verified the possibility that, differently from compound **1**, EMAC derivatives could bind the RNase H catalytic site through an interaction with the  $Mg^{2+}$  ions, measuring their spectrum of absorbance in the absence and in the presence of  $MgCl_2$ , observing no differences (Figure 2). Hence, it is possible to assume that EMAC derivatives do not inhibit the RNase H function by binding the  $Mg^{2+}$  ions in the catalytic site.

**Figure 2 here**

Next, we investigated the possible binding of EMAC compounds either in the NNRTIBP or in the RNase H allosteric site close to the NNRTIBP by studying the effect of single point mutation. In particular the activity of **EMAC2076** on Tyr181Cys and Lys103Asn mutated RT was investigated, since these mutations are commonly selected in NNRTI resistance [32]. The same mutated enzymes were evaluated using the NNRTI **EFV** and **RDS1643**, as controls (Table 2) [13]. Results showed that **EMAC2076** retains its potency of inhibition on both RT-associated functions when tested on Lys103Asn and Tyr181Cys RTs. Its behaviour is analogue to that previously reported for compound **1**: mutated residues were not essential for the interaction of inhibitor with the HIV-1 RT.

**Table 2 here**

Subsequently, we further investigated the NNRTIBP by checking if **EMAC2076** and the NNRTI **EFV** were able to simultaneously bind to RT. Hence, we performed a revised Yonetani-Theorell

model [33] that allows to discriminate between inhibitors that compete for a single binding site (and are kinetically mutually exclusive) and inhibitors that bind to two non-overlapping binding sites (and are kinetically not mutually exclusive). In this revised model, the plot of the reaction velocity reverse ( $1/v$ ) observed in the presence of different concentrations of the first inhibitor, in the absence or in the contemporaneous presence of the second inhibitor, leads to a series of lines which are parallel if the two inhibitors compete for the same binding site, whereas they intersect if the inhibitors bind to different enzyme sites. Results showed that the dual inhibitor **EMAC2076** is not kinetically mutually exclusive with **EFV** for the binding to the NNRTIBP, suggesting that both compounds can bind to RT at the same time (Figure 3). In addition, since the calculation of the interaction constant  $\alpha$ , allows to estimate the degree of binding interference of the two inhibitors [33], we calculated this constant for all three obtained curves in the presence of **EFV** with respect to the one without **EFV**. The obtained  $\alpha$  value was  $2.6 \pm 0.17$ , thus indicating a negative influence of the binding of one inhibitor with respect to the other. Overall, these results fully support the hypothesis that **EMAC2076** binds an allosteric site close-by and not overlapping with the NNRTI binding pocket. In the light of these data and considering that EMAC derivatives activity is not affected when assayed on common resistant mutants we can consider these compounds as promising hit candidates.

**Figure 3 here**

The binding mode of compound **EMAC2076** with RT HIV-1 has been further investigated by docking experiments, according to the same protocol described in our previous work [20]. The allosteric RNase H binding pocket of RT is mainly lipophilic with aromatic residues. Therefore, hydrophobic interactions play crucial role on determining anti-HIV activity. Moreover, this pocket is characterized by an L shape expanding from the region next to catalytic DP site to the NNRTIBP [34].

The obtained [EMAC2076•RT] complexes were subjected to a post-docking procedure based on energy minimization and subsequent binding free energies calculation. The free energies of binding were obtained applying molecular mechanics and continuum solvation models using the molecular mechanics Generalized Born/Surface Area (MM-GBSA) method [35].

To further validate the docking pose, the experiment was carried out also on Tyr181Cys mutated enzyme. The best docking poses (Figure 4) show that Tyr181Cys mutation did not change the ligand binding mode (Table S3 of SD).

Moreover, the evaluated interaction energies are comparable (-43.87 vs -42.89 kcal/mol). This is in agreement with the biological data (Table S3 of SD).

The best docking pose for EMAC2076 shows the molecule involved in Van-der-Waals contacts with Leu228, Val108, Pro226 side-chains. The biphenyl substituent is oriented towards NNRTIBP and stabilized by an array of aromatic  $\pi$ - $\pi$  interactions involving Tyr188, Phe227 and Trp229. However, the rigidity of this group does not allow the compound to enter more deeply in the L pocket. Stacking contacts are also possible with Tyr181Cys mutation, which was shown to confer no resistance to this inhibitor (Table 2). Interestingly, the biphenyl hydrophobic substituent orients the compound with the indolinone portion outside the pocket, while the previously reported compound **1** seems to prefer a 180° rotated orientation. This is probably due to the presence, in the case of compound **1**, of the more polar di-hydroxyphenyl moiety with respect to the lipophilic biphenyl substituent of compound EMAC2076. Such polar substituent confers a higher water affinity and flips the ligand with the thiazole portion oriented to the outer, solvent exposed, part of the enzyme cavity. Furthermore, this orientation is stabilised through a favourable  $\pi$ - $\pi$  stacking between the indolinone portion and Trp229 (Figure 4 and Table S3). However, in our opinion, the binding mode of EMAC2076 offers more space for chemical optimization, since the activity of these derivatives could be further improved with a wide variety of hydrophobic and heterocyclic substituents in position 4 of thiazole ring and by keeping the indolinone portion oriented towards

the solvent with appropriate substitutions. Indeed, the presence of an aromatic ring seems important to allow stacking interactions with the highly conserved Phe227 and Trp229 residues [36].

On the whole, the good agreement between the drug resistance mutation profile, Yonetani plot and the docking poses represents a further validation of the obtained results and corroborates the hypothesis that **EMAC2076** binds the RNase H allosteric site close-by but not overlapping with the NNRTI binding pocket.

**Figure 4 here**

#### **4. Conclusion**

The present study describes a simple method for the synthesis of indolinone derivatives. These compounds show interesting dual inhibitory activity on both RNase H and DP HIV-1 RT-associated functions, leading to inhibitors that may completely block RT activities. Biochemical and molecular modelling studies confirm that, as the hit compound **1**, also the new derivatives are able to bind an allosteric pocket that modulates both RT activities. Furthermore, mutagenesis studies helped to elucidate the mechanism of action and showed that the most active compound **EMAC2076** displays a favourable drug resistance profile since its activity is conserved on most common NNRTI resistant mutants. Molecular modelling experiments evidenced the orientation of compound **EMAC2076** in the allosteric RNase H binding pocket with the biphenyl moiety pointed towards the NNRTIBP. Since the system seems really susceptible to the nature of the aromatic substituents in the position 4 of thiazole ring, the activity could be further improved with a wide variety of substituents, and heterocyclic systems and through an accurate modulation of electronic, steric and solvation effects. Hence these new derivatives could be considered as a key step towards the design of dual DP/RNase H HIV 1 RT inhibitors.

#### **5. Experimental Section**

##### ***5.1 Material and General methods***

Starting materials and reagents were obtained from commercial suppliers and were used without purification. All melting points were determined by the capillary method on a Büchi-540 capillary melting points apparatus and are uncorrected. Electron ionization mass spectra were obtained by a Fisons QMD 1000 mass spectrometer (70 eV, 200 mA, ion source temperature 200°C). Samples were directly introduced into the ion source. Found mass values are in agreement with theoretical ones. Melting points, yield of reactions and the analytical data of derivatives are reported in Tables S1, S2, and S3 of SD.

All samples were measured in DMF-*d*<sub>7</sub> or DMSO-*d*<sub>6</sub> solvent at 278.1 K temperature on a Bruker AVANCE III 500 MHz spectrometer. Chemical shifts are reported relative to TMS ( $\delta = 0$ ) and/or referenced to the solvent in which they were measured. (In the <sup>15</sup>N chemical shift assignments we applied the spectrometer's digital reference which is calibrated to liq. NH<sub>3</sub>  $\delta = 0$  ppm.) Coupling constants *J* are expressed in hertz (Hz).

Elemental analyses were obtained on a Perkin–Elmer 240 B microanalyser. Analytical data of the synthesised compounds are in agreement within  $\pm 0.4$  % of the theoretical values. TLC chromatography was performed using silica gel plates (Merck F 254), spots were visualised by UV light.

## 5.2 Synthesis of compound EMAC 2072 (Z)-3-(2-(4-(4-chlorophenyl)thiazol-2-yl)hydrazono)indolin-2-one (general procedure)

The synthesis is accomplished by a two step procedure

### a) Synthesis of 2-(2-oxoindolin-3-ylidene)-hydrazinecarbothioamide

0,5g (3.8 mmol) of indolinone-2,3-dione and 0,35g (3.8 mmol) of thiosemicarbazide were introduced in a three necked flask and dissolved with 25 mL of 2-propanol at 50°C. 5 drops of CH<sub>3</sub>COOH were added to the mixture reaction as catalyst. After a few minutes the formation of an abundant yellow precipitate is observe. The reaction was monitored with TLC (eluent

ethylacetate:exane 7:2). After 24 hours the reaction is completed and the solid filtered. The desired compound is a yellow solid. R.f.: 0.33 (eluent ethylacetate:exane 7:2); M.P.: >250°C; Yield: 97%

<sup>1</sup>H NMR (DMF) δ(ppm): 12.72 (s; 1H); 11.34 (s; 1H); 9.21 (s; 1H); 9.05 (s; 1H); 7.66-7.64 (m; 1H); 7.42-7.34 (m; 1H); 7.17-7.10 (m; 1H); 7.06-7.02 (m; 1H)

<sup>13</sup>C NMR (DMF) δ(ppm): 180.1; 163.3; 143.1; 132.4; 131.6; 122.8; 121.1; 120.7; 111.5

<sup>15</sup>N NMR (DMF) δ(ppm): 170.0; 135.6; 110.4

b) *Synthesis of (Z)-3-(2-(4-(4-chlorophenyl)thiazol-2-yl)hydrazono)indolin-2-one EMAC 2072*

0.5g (2.3 mmol) of (Z)-1-(2-oxoindolin-3-ylidene)thiosemicarbazide and 0.54g (2.3 mol) of 2-bromo-4'-chloroacetophenone were stirred at r.t. in 30 ml of 2-propanol. After few minutes the formation of an abundant light yellow-orange precipitate was observed. The reaction was monitored by TLC (eluent exane:ethylacetate 7:2) and after 24 hours it was completed. The desired compound is a yellow-orange solid. R.f.:0.85 (eluent exane:ethylacetate 7:2); M.P.: >250°C; Yield: 73%

### 5.3. NMR Final Compounds characterisation:

5.3.1.1 *(Z)-3-(2-(4-(4-chlorophenyl)thiazol-2-yl)hydrazono)indolin-2-one (EMAC2072)*

<sup>1</sup>H NMR (DMF-d7) δ(ppm): 13.55 (s, 1H); 11.43 (s; 1H); 8.07-8.02 (m; 2H); 7.82 (s; 1H); 7.63 (dm; *J*=7.6 Hz; 1H); 7.58-7.53 (m; 2H); 7.41 (td; *J*=7.6 Hz; 1.1 Hz; 1H); 7.16 (td; *J*=7.6 Hz; 1.0 Hz; 1H); 7.10 (dm; *J*=7.6 Hz; 1H)

<sup>13</sup>C NMR (DMF-d7) δ(ppm): 166.9; 164.0; 150.6; 142.1; 133.6; 133.1; 132.7; 130.9; 129.2; 127.9; 122.8; 120.5; 120.3; 111.5; 107.7

<sup>15</sup>N NMR (DMF-d7) δ(ppm): 156.2; 135.7

5.3.2 *(Z)-3-(2-(4-(4-fluorophenyl)thiazol-2-yl)hydrazono)indolin-2-one (EMAC2073)*

<sup>1</sup>H NMR (DMSO-d6) δ(ppm): 13.33 (s; 1H); 11.25 (s; 1H); 7.97-7.90 (m; 2H); 7.60 (s; 1H); 7.53 (dm; *J*= 7.5 Hz; 1H); 7.34 (tm; *J*= 7.5 Hz; 1H); 7.29-7.17 (m; 2H); 7.09 (tm; *J*= 7.5 Hz; 1H); 6.99-6.92 (m; 1H)

$^{13}\text{C}$  NMR (DMSO- $d_6$ )  $\delta$ (ppm): 166.4; 163.2; 161.9 (d;  $J$ = 244.6 Hz); 150.0; 141.3; 132.2; 130.6; 130.5; 127.8 (d;  $J$ = 8.3 Hz) 122.4; 119.9; 119.8; 115.6 (d;  $J$ = 21.6 Hz); 111.1; 106.6

$^{15}\text{N}$  NMR (DMSO- $d_6$ )  $\delta$ (ppm): 137.1

### 5.3.3 (Z)-3-(2-(4-(4-bromophenyl)thiazol-2-yl)hydrazono)indolin-2-one (EMAC2074)

$^1\text{H}$  NMR (DMF- $d_7$ )  $\delta$ (ppm): 13.53 (s; 1H); 11.42 (s; 1H); 7.99-7.93 (m; 2H); 7.82 (s; 1H); 7.71-7.65 (m; 2H); 7.61 (dm;  $J$ = 7.6 Hz; 1H); 7.39 (tm;  $J$ = 7.6 Hz; 1H); 7.14 (tm;  $J$ = 7.6 Hz; 1H); 7.08 (dm;  $J$ = 7.6 Hz; 1H)

$^{13}\text{C}$  NMR (DMF- $d_7$ )  $\delta$ (ppm): 167.0; 164.0; 150.7; 142.1; 133.9; 132.7; 132.1; 130.9; 128.1; 122.8; 121.6; 120.5; 120.3; 111.5; 107.8

$^{15}\text{N}$  NMR (DMF- $d_7$ )  $\delta$ (ppm): 156.1; 135.7

### 5.3.4 (Z)-3-(2-(4-(4-nitrophenyl)thiazol-2-yl)hydrazono)indolin-2-one (EMAC2075)

$^1\text{H}$  NMR (DMF- $d_7$ )  $\delta$ (ppm): 13.55 (s; 1H); 11.42 (s; 1H); 8.38-8.32 (m; 2H); 8.30-8.24 (m; 2H); 8.12 (s; 1H); 7.62 (dm;  $J$ = 7.7 Hz; 1H); 7.40 (td;  $J$ = 7.7 Hz; 1.2 Hz; 1H); 7.15 (td;  $J$ = 7.7 Hz; 0.7 Hz; 1H); 7.08 (dm;  $J$ = 7.7 Hz; 1H)

$^{13}\text{C}$  NMR (DMF- $d_7$ )  $\delta$ (ppm): 167.3; 163.9; 149.7; 147.2; 142.2; 140.7; 133.1; 131.1; 127.0; 124.5; 122.9; 120.4; 120.3; 111.6; 111.6

$^{15}\text{N}$  NMR (DMF- $d_7$ )  $\delta$ (ppm): 155.8; 135.7

### 5.3.5 (Z)-3-{2-[4-(4-biphenyl)-thiazol-2-yl]hydrazono}indolin-2-one (EMAC2076)

$^1\text{H}$  NMR (DMF- $d_7$ )  $\delta$ (ppm): 13.56 (s; 1H); 11.41 (s; 1H); 8.13-8.08 (m; 2H); 7.85-7.75 (m; 5H); 7.63 (d;  $J$ = 7.6 Hz; 1H); 7.55-7.49 (m; 2H); 7.44-7.36 (m; 2H); 7.15 (tm;  $J$ = 7.6 Hz; 1H); 7.08 (dm;  $J$ = 7.6 Hz; 1H)

$^{13}\text{C}$  NMR (DMF- $d_7$ )  $\delta$ (ppm): 166.8; 164.0; 151.6; 142.1; 140.4; 140.3; 133.8; 132.6; 130.9; 129.4; 127.9; 127.4; 127.0; 126.7; 122.8; 120.5; 120.2; 111.5; 107.1

$^{15}\text{N}$  NMR (DMF-d7)  $\delta$ (ppm): 156.5; 135.7

5.3.6 (Z)-3-(2-(4-(2,4-difluorophenyl)thiazol-2-yl)hydrazono)indolin-2-one (**EMAC2077**)

$^1\text{H}$  NMR (DMF-d7)  $\delta$ (ppm): 13.52 (s; 1H); 11.39 (s; 1H); 8.23-8.14 (m; 1H); 7.62 (d;  $J$ = 7.6 Hz; 1H); 7.58(d;  $J$ = 2.4 Hz; 1H); 7.45-7.36 (m; 2H); 7.25 (td;  $J$ = 8.5 Hz; 2.5 Hz; 1H); 7.15 (td;  $J$ = 7.6 Hz; 0.7 Hz; 1H); 7.07 (dm;  $J$ = 7.6 Hz; 1H)

$^{13}\text{C}$  NMR (DMF-d7)  $\delta$ (ppm): 166.4; 164.0; 162.3 (dd;  $J$ = 248.0 Hz; 12.4 Hz); 160.4 (dd;  $J$ = 251.9 Hz; 12.3 Hz); 144.7 (dd;  $J$ = 2.6 Hz; 0.9 Hz); 142.1; 132.8; 131.2 (dd;  $J$ = 9.6Hz; 4.8 Hz); 131.0; 122.9; 120.5; 120.3; 119.1 (dd;  $J$ = 11.3Hz; 3.7 Hz); 112.3 (dd;  $J$ = 21.4Hz; 3.4 Hz); 111.5; 111.2 (d;  $J$ = 15.0 Hz); 104.9 (t;  $J$ = 26.5 Hz)

$^{15}\text{N}$  NMR (DMF-d7)  $\delta$ (ppm): 155.9; 135.5

5.3.7 (Z)-3-(2-(4-(3-nitrophenyl)thiazol-2-yl)hydrazono)indolin-2-one (**EMAC2078**)

$^1\text{H}$  NMR (DMF-d7)  $\delta$ (ppm): 13.57 (s; 1H); 11.41 (s; 1H); 8.84-8.76 (m; 1H); 8.46 (dm;  $J$ = 8.1 Hz; 1H); 8.26 (dm;  $J$ = 8.1 Hz; 1H); 8.09 (s; 1H); 7.80 (t;  $J$ = 8.1 Hz; 1H); 7.63 (d;  $J$ = 7.6 Hz; 1H); 7.41 (tm;  $J$ = 7.6 Hz; 1H); 7.15 (tm;  $J$ = 7.6 Hz; 1H); 7.08 (dm;  $J$ = 7.6 Hz; 1H)

$^{13}\text{C}$  NMR (DMF-d7)  $\delta$ (ppm): 167.3; 164.0; 149.5; 149.0; 142.2; 136.3; 133.0; 132.2; 131.0; 130.7; 122.9; 122.9; 120.6; 120.4; 120.3; 111.5; 109.6

$^{15}\text{N}$  NMR (DMF-d7)  $\delta$ (ppm): 155.9; 135.5

5.3.8 (Z)-3-(2-(4-*p*-tolylthiazol-2-yl)hydrazono)indolin-2-one (**EMAC2079**)

$^1\text{H}$  NMR (DMF-d7)  $\delta$ (ppm): 13.53 (s; 1H); 11.38 (s; 1H); 7.91-7.86 (m; 2H); 7.66 (s; 1H); 7.62 (d;  $J$ = 7.6 Hz; 1H); 7.39 (td;  $J$ = 7.6 Hz; 1.2 Hz; 1H); 7.30-7.25 (m; 2H); 7.15 (td;  $J$ = 7.6 Hz; 0.8 Hz; 1H); 7.07 (dm;  $J$ = 7.6 Hz; 1H); 2.35 (s; 3H)

$^{13}\text{C}$  NMR (DMF-d7)  $\delta$ (ppm): 166.6; 164.0; 152.0; 142.0; 138.0; 132.4; 132.1; 130.8; 129.7; 126.1; 122.8; 120.5; 120.2; 111.5; 106.0; 20.8

$^{15}\text{N}$  NMR (DMF-d7)  $\delta$ (ppm): 156.4; 135.5

5.3.9 (Z)-3-(2-(4-(4-methoxyphenyl)thiazol-2-yl)hydrazono)indolin-2-one (**EMAC2080**)

$^1\text{H}$  NMR (DMF-d7)  $\delta$ (ppm): 13.53 (s; 1H); 11.40 (s; 1H); 7.95-7.91 (m; 2H); 7.63-7.59 (dm;  $J= 7.7$  Hz; 1H); 7.56 (s; 1H); 7.39 (td;  $J= 7.7$  Hz; 1.1 Hz; 1H); 7.15 (td;  $J= 7.7$  Hz; 1.0 Hz; 1H); 7.08 (dm;  $J= 7.7$  Hz; 1H); 7.06-7.02 (m, 2H); 3.85 (s; 3H)

$^{13}\text{C}$  NMR (DMF-d7)  $\delta$ (ppm): 166.6; 164.0; 159.9; 151.8; 142.0; 132.4; 130.8; 127.5; 127.5; 122.8; 120.5; 120.2; 114.3; 111.5; 104.7; 55.3

$^{15}\text{N}$  NMR (DMF-d7)  $\delta$ (ppm): 156.6; 135.6

5.3.10 (Z)-3-(2-(4-phenylthiazol-2-yl)hydrazono)indolin-2-one (**EMAC2081**)

$^1\text{H}$  NMR (DMF-d7)  $\delta$ (ppm): 13.54 (s; 1H); 11.41 (s; 1H); 8.01-7.97 (m; 2H); 7.74 (s; 1H); 7.62 (dm;  $J= 7.7$  Hz; 1H); 7.49-7.44 (m; 2H); 7.42-7.34 (m; 2H); 7.17-7.10 (m; 1H); 7.08 (dm;  $J= 7.7$  Hz; 1H)

$^{13}\text{C}$  NMR (DMF-d7)  $\delta$ (ppm): 166.8; 164.0; 151.9; 142.1; 134.7; 132.6; 130.9; 129.1; 128.3; 126.1; 122.8; 120.5; 120.2; 111.5; 106.9

$^{15}\text{N}$  NMR (DMF-d7)  $\delta$ (ppm): 156.2; 135.6

5.3.11 (Z)-3-(2-(4-(2,4-dichlorophenyl)thiazol-2-yl)hydrazono)indolin-2-one (**EMAC2082**)

$^1\text{H}$  NMR (DMF-d7)  $\delta$ (ppm): 13.51 (s; 1H); 11.39 (s; 1H); 8.05 (d;  $J= 8.5$  Hz; 1H); 7.85 (s; 1H); 7.75 (d;  $J= 2.2$  Hz; 1H); 7.63 (dm;  $J= 7.6$  Hz; 1H); 7.58 (dd;  $J= 8.5$  Hz; 2.2 Hz; 1H); 7.40 (td;  $J= 7.6$  Hz; 1.2 Hz; 1H); 7.15 (td;  $J= 7.6$  Hz; 1.0 Hz; 1H); 7.07 (dm;  $J= 7.6$  Hz; 1H)

$^{13}\text{C}$  NMR (DMF-d7)  $\delta$ (ppm): 166.1; 164.0; 147.1; 142.1; 133.6; 132.6; 132.9; 132.2; 132.1; 131.0; 130.4; 128.1; 122.9; 120.5; 120.3; 112.9; 111.5

$^{15}\text{N}$  NMR (DMF-d7)  $\delta$ (ppm): 155.6; 135.5

## 5.4 Biochemistry studies

### 5.4.1 HIV-1 RT purification.

Heterodimeric RT was expressed essentially as described [37].

### 5.4.2 HIV-1 RT-associated DNA polymerase-independent RNase H activity determination.

The HIV RT-associated RNase H activity was measured as described [38]. Briefly, 20 ng of HIV-1 wt Reverse Transcriptase was incubated for 1 h at 37 °C in 100 µL reaction volume containing 50 mM Tris HCl pH 7.8, 6 mM MgCl<sub>2</sub>, 1 mM dithiothreitol (DTT), 80 mM KCl, 250nM hybrid RNA/DNA (5'-GTTTTCTTTTCCCCCTGAC-3'-Fluorescein, 5'-CAAAGAAAAGGGGGGACUG-3'-Dabcyl). Reactions were stopped by addition of EDTA and products were measured with a with a PerkinElmer Victor 3 multilabel counter plate reader at excitation- emission wavelength of 490/528 nm.

### 5.4.3 HIV-1 RT-associated RNA dependent DNA polymerase activity determination.

The HIV-1 RT-associated RNA-Dependent DP activity was measured as previously described [39]. Briefly, 20 ng of HIV-1 wt Reverse Transcriptase was incubated for 30 min at 37 °C in 25 µL volume containing 60 mM Tris-HCl pH 8.1, 8 mM MgCl<sub>2</sub>, 60 mM KCl, 13 mM DTT, 2.5 µM poly(A)-oligo(dT), 100 µM dTTP. Enzymatic reaction was stopped by addition of EDTA. Reaction products were detected by picogreen addition and measured with a PerkinElmer Victor 3 multilabel counter plate reader at excitation- emission wavelength of 502/523 nm.

Chemical reagents were purchased from Sigma-Aldrich srl. RNA- DNA labeled sequences were purchased from Metabion international AG.

### 5.4.4 The Yonetani-Theorell analysis.

The Yonetani-Theorell analysis was performed according to the official protocol [33]

The calculation of the interaction constant  $\alpha$ , allows to estimate the degree of interference of the two inhibitors for the binding, was performed according to the following equation, assuming that  $K_{EFV}$

= IC<sub>50</sub> for non-competitive inhibitors in accordance with Prusoff–Cheng equation [40] and equal to 12 nM in our system.

$$\frac{\text{slope with EFV}}{\text{slope without EFV}} = 1 + \frac{[\text{nM EFV}]}{\alpha K_{\text{EFV}}}$$

## 5.5 Molecular Modeling

### 5.3.1 Ligand preparation.

The ligand was built within Maestro GUI and its geometry was optimized. The lowest energy conformer was considered for the following studies. This was obtained with MacroModel version 7.2 [41], considering MMFFs [42] as force field and solvent effects by adopting the implicit solvation model Generalized Born/Surface Area (GB/SA) water [43]. The simulation was performed allowing 1000 steps Monte Carlo analysis with Polak-Ribier Coniugate Gradient (PRCG) method and a convergence criterion of 0.05 kcal/(molÅ).

### 5.5.2. Protein Preparation.

The atomic coordinates of the protein with pdb code 3LP2 [17] were imported into the Maestro module available in the Schrödinger package[44]. The protein was further optimized using the Protein Preparation Wizard[44].

### 5.5.3 Docking and post-docking procedure.

The docking experiments were performed as described in our previous work [20] applying Quantum Mechanic-polarized ligand docking (QPLD) [45]. In order to better take into account the induced fit phenomena, the most energy favoured generated complexes were fully optimized with the AMBER\* united atoms force field [46] in GB/SA implicit water [43], setting 10000 steps iterations analysis with Polak-Ribier Coniugate Gradient (PRCG) method and a convergence criterion of 0.1 kcal/(molÅ). Analysis of the results of the complex minimization was carried out taking into account the state equations (free energy of complex formation) computed at 300 K, applying molecular mechanics and continuum solvation models with the molecular mechanics

generalized Born [35]. The resulting complexes were considered for the binding modes graphical analysis with Pymol [47] and Maestro [44].

### Acknowledgements

This work was supported by RAS grant LR 7/2007 CRP2\_450, CRP-24915, and Istituto Superiore di Sanità grant RF-PAD-2009-1304305 n. 40H98. Rita Meleddu PhD grant was founded by Fondazione Banco di Sardegna.

### Appendix. Supplementary material

Supplementary material associated with this article: Chemical-physical, spectroscopic and analytical data of derivatives **EMAC2072-2082**, NOE effect for E and Z configuration, docking scores, post-docking energies and main active site residues interactions, NMR spectra, MS fragmentation. Supplementary material associated with this article can be found, in the online version, at...

### References

- [1] P. Zhan, X. Liu, Z. Li, C. Pannecouque, E. De Clercq, Design strategies of novel NNRTIs to overcome drug resistance, *Curr. Med. Chem.*, 16 (2009) 3903-3917.
- [2] R. Morphy, Z. Rankovic, Designed multiple ligands. An emerging drug discovery paradigm, *J. Med. Chem.*, 48 (2005) 6523-6543.
- [3] M.S. Hirsch, Initiating therapy: When to start, what to use, *J. Infect. Dis.*, 197 (2008) S252-S260.
- [4] E. Tramontano, HIV-1 RNase H: recent progress in an exciting, yet little explored, drug target, *Mini Rev. Med. Chem.*, 6 (2006) 727-737.
- [5] K. Klumpp, T. Mirzadegan, Recent progress in the design of small molecule inhibitors of HIV RNase H, *Curr. Pharm. Des.*, 12 (2006) 1909-1922.

- [6] A. Corona, F. Esposito, E. Tramontano, Can the ever-promising target HIV reverse transcriptase-associated RNase H become a success story for drug development?, *Future Vir.*, 9 (2014) 445-448.
- [7] A. Corona, T. Masaoka, G. Tocco, E. Tramontano, S.F.J. Le Grice, Active site and allosteric inhibitors of the ribonuclease H activity of HIV reverse transcriptase, *Future Med. Chem.*, 5 (2013) 2127-2139.
- [8] D.M. Himmel, K.A. Maegley, T.A. Pauly, J.D. Bauman, K. Das, C. Dharia, A.D. Clark Jr, K. Ryan, M.J. Hickey, R.A. Love, S.H. Hughes, S. Bergqvist, E. Arnold, Structure of HIV-1 reverse transcriptase with the inhibitor  $\beta$ -Thujaplicinol bound at the RNase H active site, *Structure*, 17 (2009) 1625-1635.
- [9] S. Chung, D.M. Himmel, J.-K. Jiang, K. Wojtak, J.D. Bauman, J.W. Rausch, J.A. Wilson, J.A. Beutler, C.J. Thomas, E. Arnold, S.F.J. Le Grice, Synthesis, activity, and structural analysis of novel  $\alpha$ -Hydroxytropolone inhibitors of human immunodeficiency virus reverse transcriptase-associated Ribonuclease H, *J. Med. Chem.*, 54 (2011) 4462-4473.
- [10] T.A. Kirschberg, M. Balakrishnan, N.H. Squires, T. Barnes, K.M. Brendza, X. Chen, E.J. Eisenberg, W. Jin, N. Kutty, S. Leavitt, A. Liclican, Q. Liu, X. Liu, J. Mak, J.K. Perry, M. Wang, W.J. Watkins, E.B. Lansdon, RNase H active site inhibitors of human immunodeficiency virus type 1 reverse transcriptase: Design, biochemical activity, and structural information, *J. Med. Chem.*, 52 (2009) 5781-5784.
- [11] E.B. Lansdon, Q. Liu, S.A. Leavitt, M. Balakrishnan, J.K. Perry, C. Lancaster-Moyer, N. Kutty, X. Liu, N.H. Squires, W.J. Watkins, T.A. Kirschberg, Structural and binding analysis of pyrimidinol carboxylic acid and N-hydroxy quinazolinedione HIV-1 RNase H inhibitors, *Antimicrob. Agents Chemother.*, 55 (2011) 2905-2915.
- [12] J.Q. Hang, S. Rajendran, Y. Yang, Y. Li, P. Wong Kai In, H. Overton, K.E.B. Parkes, N. Cammack, J.A. Martin, K. Klumpp, Activity of the isolated HIV RNase H domain and specific inhibition by N-hydroxyimides, *Biochem. Biophys. Res. Commun.*, 317 (2004) 321-329.

- [13] E. Tramontano, F. Esposito, R. Badas, R. Di Santo, R. Costi, P. La Colla, 6-[1-(4-Fluorophenyl)methyl-1H-pyrrol-2-yl)]-2,4-dioxo-5-hexenoic acid ethyl ester a novel diketo acid derivative which selectively inhibits the HIV-1 viral replication in cell culture and the ribonuclease H activity in vitro, *Antivir. Res.*, 65 (2005) 117-124.
- [14] R. Costi, M. Métirot, F. Esposito, G. Cuzzucoli Crucitti, L. Pescatori, A. Messori, L. Scipione, S. Tortorella, L. Zinzula, E. Novellino, Y. Pommier, E. Tramontano, C. Marchand, R. Di Santo, 6-(1-Benzyl-1H-pyrrol-2-yl)-2,4-dioxo-5-hexenoic acids as dual inhibitors of recombinant HIV-1 integrase and ribonuclease h, synthesized by a parallel synthesis approach, *J. Med. Chem.*, 56 (2013) 8588-8598.
- [15] F. Esposito, E. Tramontano, Past and future. Current drugs targeting HIV-1 integrase and reverse transcriptase-associated ribonuclease H activity: single and dual active site inhibitors, *Antivir. Chem. Chemother.*, 23 (2014) 129-144.
- [16] D.M. Himmel, S.G. Sarafianos, S. Dharmasena, M.M. Hossain, K. McCoy-Simandle, T. Ilina, A.D. Clark, Jr., J.L. Knight, J.G. Julias, P.K. Clark, K. Krogh-Jespersen, R.M. Levy, S.H. Hughes, M.A. Parniak, E. Arnold, HIV-1 reverse transcriptase structure with RNase H inhibitor dihydroxy benzoyl naphthyl hydrazone bound at a novel site, *ACS Chem. Biol.*, 1 (2006) 702-712.
- [17] H.P. Su, Y. Yan, G.S. Prasad, R.F. Smith, C.L. Daniels, P.D. Abeywickrema, J.C. Reid, H.M. Loughran, M. Kornienko, S. Sharma, J.A. Grobler, B. Xu, V. Sardana, T.J. Allison, P.D. Williams, P.L. Darke, D.J. Hazuda, S. Munshi, Structural basis for the inhibition of RNase H activity of HIV-1 reverse transcriptase by RNase H active site-directed inhibitors, *J. Virol.*, 84 (2010) 7625-7633.
- [18] F. Esposito, T. Kharlamova, S. Distinto, L. Zinzula, Y.-C. Cheng, G. Dutschman, G. Floris, P. Markt, A. Corona, E. Tramontano, Alizarine derivatives as new dual inhibitors of the HIV-1 reverse transcriptase-associated DNA polymerase and RNase H activities effective also on the RNase H activity of non-nucleoside resistant reverse transcriptases, *FEBS J.*, 278 (2011) 1444-1457.
- [19] R. Meleddu, V. Cannas, S. Distinto, G. Sarais, C. DelVecchio, F. Esposito, G. Bianco, A. Corona, F. Cottiglia, S. Alcaro, C. Parolin, A. Artese, D. Scalise, M. Fresta, A. Arridu, F. Ortuso, E.

Maccioni, E. Tramontano, Design, synthesis, and biological evaluation of 1,3-diarylpropenones as dual inhibitors of HIV-1 reverse transcriptase, *ChemMedChem*, 9 (2014) 1869-1879.

[20] S. Distinto, F. Esposito, J. Kirchmair, M.C. Cardia, M. Gaspari, E. Maccioni, S. Alcaro, P. Markt, G. Wolber, L. Zinzula, E. Tramontano, Identification of HIV-1 reverse transcriptase dual inhibitors by a combined shape-, 2D-fingerprint- and pharmacophore-based virtual screening approach, *Eur. J. Med. Chem.*, 50 (2012) 216-229.

[21] E. Tramontano, R. Di Santo, HIV-1 RT-associated RNase H function inhibitors: recent advances in drug development, *Curr. Med. Chem.*, 17 (2010) 2837-2853.

[22] T. Kharlamova, F. Esposito, L. Zinzula, G. Floris, C. Yung-Chi, G.E. Dutschman, E. Tramontano, Inhibition of HIV-1 ribonuclease H activity by novel frangula-emodine derivatives, *Med. Chem.*, 5 (2009) 398-410.

[23] S.J. Taylor, A.K. Padyana, A. Abeywardane, S. Liang, M.-H. Hao, S. De Lombaert, J. Proudfoot, B.S. Farmer, X. Li, B. Collins, L. Martin, D.R. Albaugh, M. Hill-Drzewi, S.S. Pullen, H. Takahashi, Discovery of potent, selective chymase inhibitors via fragment linking strategies, *J. Med. Chem.*, 56 (2013) 4465-4481.

[24] R. Laufer, B. Forrest, S.-W. Li, Y. Liu, P. Sampson, L. Edwards, Y. Lang, D.E. Awrey, G. Mao, O. Plotnikova, G. Leung, R. Hodgson, I. Beletskaya, J.M. Mason, X. Luo, X. Wei, Y. Yao, M. Feher, F. Ban, R. Kiarash, E. Green, T.W. Mak, G. Pan, H.W. Pauls, The discovery of PLK4 inhibitors: (E)-3-((1H-indazol-6-yl)methylene)indolin-2-ones as novel antiproliferative agents, *J. Med. Chem.*, 56 (2013) 6069-6087.

[25] J. Yuan, S. Venkatraman, Y. Zheng, B.M. McKeever, L.W. Dillard, S.B. Singh, Structure-based design of  $\beta$ -site APP cleaving enzyme 1 (BACE1) inhibitors for the treatment of Alzheimer's disease, *J. Med. Chem.*, 56 (2013) 4156-4180.

[26] S. Crosignani, C. Jorand-Lebrun, P. Page, G. Campbell, V. Colovray, M. Missotten, Y. Humbert, C. Cleva, J.-F. Arrighi, M. Gaudet, Z. Johnson, P. Ferro, A. Chollet, Optimization of the

central core of indolinone–acetic acid-based CRTH2 (DP2) receptor antagonists, *ACS Med. Chem. Lett.*, 2 (2011) 644-649.

[27] S. Distinto, M. Yáñez, S. Alcaro, M.C. Cardia, M. Gaspari, M.L. Sanna, R. Meleddu, F. Ortuso, J. Kirchmair, P. Markt, A. Bolasco, G. Wolber, D. Secci, E. Maccioni, Synthesis and biological assessment of novel 2-thiazolylylhydrazones and computational analysis of their recognition by monoamine oxidase B, *Eur. J. Med. Chem.*, 48 (2012) 284-295.

[28] V.U. Jeankumar, J. Renuka, P. Santosh, V. Soni, J.P. Sridevi, P. Suryadevara, P. Yogeewari, D. Sriram, Thiazole–aminopiperidine hybrid analogues: Design and synthesis of novel *Mycobacterium tuberculosis* GyrB inhibitors, *Eur. J. Med. Chem.*, 70 (2013) 143-153.

[29] P. Makam, R. Kankanala, A. Prakash, T. Kannan, 2-(2-Hydrazinyl)thiazole derivatives: Design, synthesis and in vitro antimycobacterial studies, *Eur. J. Med. Chem.*, 69 (2013) 564-576.

[30] F. Chimenti, B. Bizzarri, E. Maccioni, D. Secci, A. Bolasco, R. Fioravanti, P. Chimenti, A. Granese, S. Carradori, D. Rivanera, D. Lilli, A. Zicari, S. Distinto, Synthesis and in vitro activity of 2-thiazolylylhydrazone derivatives compared with the activity of clotrimazole against clinical isolates of *Candida* spp, *Bioorg. Med. Chem. Lett.*, 17 (2007) 4635-4640.

[31] L. Xiaoyun, L. Xiaobo, W. Baojie, G.F. Scott, C. Lili, Z. Changlin, Y. Qidong, Synthesis and evaluation of antitubercular and antibacterial activities of new 4 - (2,6 - dichlorobenzyloxy)phenyl thiazole, oxazole and imidazole derivatives. Part 2, *Eur. J. Med. Chem.*, 49 (2012) 164-171.

[32] Y. Mehellou, E. De Clercq, Twenty-six years of anti-hiv drug discovery: Where do we stand and where do we go?, *J. Med. Chem.*, 53 (2009) 521-538.

[33] T. Yonetani, The Yonetani-Theorell graphical method for examining overlapping subsites of enzyme active centers, *Methods Enzymol.*, 87 (1982) 500-509.

[34] S. Distinto, E. Maccioni, R. Meleddu, A. Corona, S. Alcaro, E. Tramontano, Molecular aspects of the RT/drug interactions. Perspective of dual inhibitors, *Curr. Pharm. Des.*, 19 (2013) 1850-1859.

[35] P.A. Kollman, I. Massova, C. Reyes, B. Kuhn, S. Huo, L. Chong, M. Lee, T. Lee, Y. Duan, W. Wang, O. Donini, P. Cieplak, J. Srinivasan, D.A. Case, T.E. Cheatham, Calculating structures and

free energies of complex molecules: Combining molecular mechanics and continuum models, *Acc. Chem. Res.*, 33 (2000) 889-897.

[36] H. Pelemans, R. Esnouf, E. De Clercq, J. Balzarini, Mutational analysis of Trp-229 of human immunodeficiency virus type 1 reverse transcriptase (RT) identifies this amino acid residue as a prime target for the rational design of new non-nucleoside RT inhibitors, *Mol. Pharmacol.*, 57 (2000) 954-960.

[37] F. Esposito, C. Sanna, C. Del Vecchio, V. Cannas, A. Venditti, A. Corona, A. Bianco, A.M. Serrilli, L. Guarcini, C. Parolin, M. Ballero, E. Tramontano, Hypericum hircinum L. components as new single-molecule inhibitors of both HIV-1 reverse transcriptase-associated DNA polymerase and ribonuclease H activities, *Pathogens and Disease*, 68 (2013) 116-124.

[38] A. Corona, F.S. Di Leva, S. Thierry, L. Pescatori, G. Cuzzucoli Crucitti, F. Subra, O. Delelis, F. Esposito, G. Rigogliuso, R. Costi, S. Cosconati, E. Novellino, R. Di Santo, E. Tramontano, Identification of highly conserved residues involved in the inhibition of the HIV-1 ribonuclease H function by diketoacid derivatives, *Antimicrob. Agents Chemother.*, (2014) *In press*.

[39] V. Suchaud, F. Bailly, C. Lion, E. Tramontano, F. Esposito, A. Corona, F. Christ, Z. Debyser, P. Cotelle, Development of a series of 3-hydroxyquinolin-2(1H)-ones as selective inhibitors of HIV-1 reverse transcriptase associated RNase H activity, *Bioorg. Med. Chem. Lett.*, 22 (2012) 3988-3992.

[40] Y. Cheng, W.H. Prusoff, Relationship between the inhibition constant ( $K_1$ ) and the concentration of inhibitor which causes 50 per cent inhibition ( $I_{50}$ ) of an enzymatic reaction, *Biochem. Pharmacol.*, 22 (1973) 3099-3108.

[41] F. Mohamadi, N.G.J. Richards, W.C. Guida, R. Liskamp, M. Lipton, C. Caufield, G. Chang, T. Hendrickson, W.C. Still, Macromodel—an integrated software system for modeling organic and bioorganic molecules using molecular mechanics, *J. Comput. Chem.*, 11 (1990) 440-467.

[42] T. Halgren, Merck molecular force field. II. MMFF94 van der Waals and electrostatic parameters for intermolecular interactions, *J. Comput. Chem.*, 17 (1996) 520-552.

- [43] W.C. Still, A. Tempczyk, R.C. Hawley, T. Hendrickson, Semianalytical treatment of solvation for molecular mechanics and dynamics, *J. Am. Chem. Soc.*, 112 (1990) 6127-6129.
- [44] Schrödinger LLC., Maestro GUI, in, New York, NY, USA, 2013.
- [45] Schrödinger LLC., QMPolarized protocol, in: Schrodinger Suite, New York, NY, USA.
- [46] D.Q. McDonald, W.C. Still, AMBER torsional parameters for the peptide backbone, *Tetrahedron Lett.*, 33 (1992) 7743-7746.
- [47] PyMOL, in, Molecular Graphics System Schrödinger, LLC.

## Captions

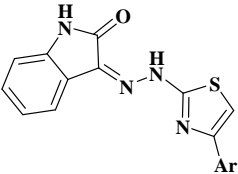
**Figure 1.** Schematic representation of **compound 1** and new derivatives.

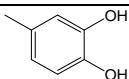
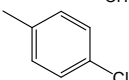
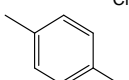
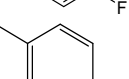
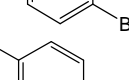
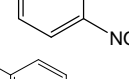
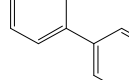
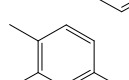
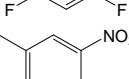
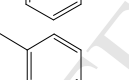
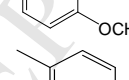
**Scheme 1.** Synthesis of (*Z*)-3-(2-(4-arylthiazol-2-yl)hydrazono)indolin-2-one derivatives **EMAC 2072-2082**. Reagents and solvents: (i) 2-propanol, AcOH; (ii) 2-propanol, room temperature (r.t).

**Figure 2.** Effect of MgCl<sub>2</sub> on the spectrum of absorbance of RHIs. Chelation of Mg<sup>2+</sup> by **RDS1643** (panel A), **Compound 1** (panel B) and **EMAC2076** (panel C). UV-vis spectrum was measured with compound alone (unbroken line) or in the presence of 6 mM MgCl<sub>2</sub> (dotted line).

**Figure 3.** Yonetani–Theorell plot of the combination of **EMAC7026** and **EFV** on the HIV-1 RT RDDP activity. HIV-1 RT was incubated in the presence of **EMAC7026** alone (●) or in presence different concentrations of **EFV**: 2 nM (▼), 8 nM (■), 16 nM (□).

**Figure 4.** Putative binding mode of a) **compound 1** –wtRT HIV-1, and d) **EMAC2076**-wt RT HIV-1; g) **EMAC2076**- Tyr181Cys-RT HIV-1; b) e) h) 2D representation of compound and binding pocket interacting residues; c) f) i) Residues involved in the complex stabilization sorted by number of contacts between ligand and receptor.

**Table 1.** EMAC derivatives effects on the HIV-1 RT-associated functions


Compound	Ar	RNase H <sup>a</sup> IC <sub>50</sub> (μM)	DP <sup>b</sup> IC <sub>50</sub> (μM)	<sup>c</sup> SpI
<b>1</b>		3.2 ± 1.2	0.9 ± 0.3	3.5
<b>EMAC2072</b>		10.6 ± 0.8	20.0 ± 6.0	0.53
<b>EMAC2073</b>		6.4 ± 1.5	23.9 ± 5.7	0.26
<b>EMAC2074</b>		14.9 ± 2.8	81.0 ± 15	0.18
<b>EMAC2075</b>		2.9 ± 0.8	34.0 ± 5	0.08
<b>EMAC2076</b>		2.5 ± 0.4	22.0 ± 1	0.11
<b>EMAC2077</b>		2.6 ± 0.5	18.5 ± 2.5	0.14
<b>EMAC2078</b>		2.8 ± 0.8	13.0 ± 5	0.21
<b>EMAC2079</b>		9.0 ± 0.9	45.0 ± 2.5	0.20
<b>EMAC2080</b>		4.7 ± 0.5	26.0 ± 5	0.18
<b>EMAC2081</b>		100	71.6 ± 16	1.3
<b>EMAC2082</b>		3.9 ± 1.5	19.5 ± 2.5	0.20
<b>Efavirenz</b>		ND <sup>d</sup>	0.012 ± 0.003	
<b>RDS1643</b>		10.1 ± 2.2	ND	

<sup>a</sup>Compound concentration required to reduce the HIV-1 RT-associated RNase H activity by 50%;

<sup>b</sup>Compound concentration required to reduce the HIV-1 RT-associated RNA-dependent DNA polymerase activity by 50%;

<sup>c</sup>Specificity Index: ratio between compound concentration required to reduce the HIV-1 RT-associated RNase H activity by 50% and compound concentration required to reduce the HIV-1 RT-associated DP activity by 50% (IC<sub>50</sub> RNase H/IC<sub>50</sub> DP);

<sup>d</sup>ND, not done.

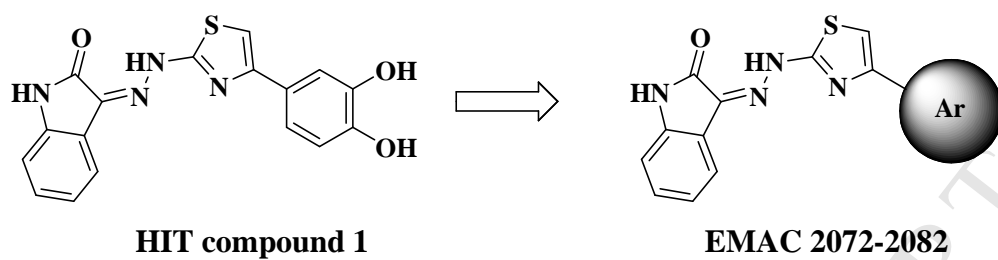
**Table 2:** Inhibition of wild-type HIV-1 and the mutants HIV-1 RT associated activities by EMAC2076 expressed as IC<sub>50</sub> (μM)

Compound	HIV-1 wt RT		HIV-1 Tyr181Cys RT		HIV-1 Lys103Asn RT	
	RNase H <sup>a</sup>	DP <sup>b</sup>	RNase H <sup>a</sup>	DP <sup>b</sup>	RNase H <sup>a</sup>	DP <sup>b</sup>
<b>EMAC2076</b>	2.5 ± 0.4	22.0 ± 1	2.7 ± 0.8	15.4 ± 2.3	3.42 ± 0.9	18.8 ± 2.7
<b>RDS1643</b>	10.1 ± 2.2	ND <sup>c</sup>	9.6 ± 1.8	ND <sup>c</sup>	9.2 ± 0.9	ND
<b>Efavirenz</b>	ND <sup>c</sup>	0.012 ± 0.003	ND <sup>c</sup>	0.680 ± 0.200	ND	0.280 ± 0.070

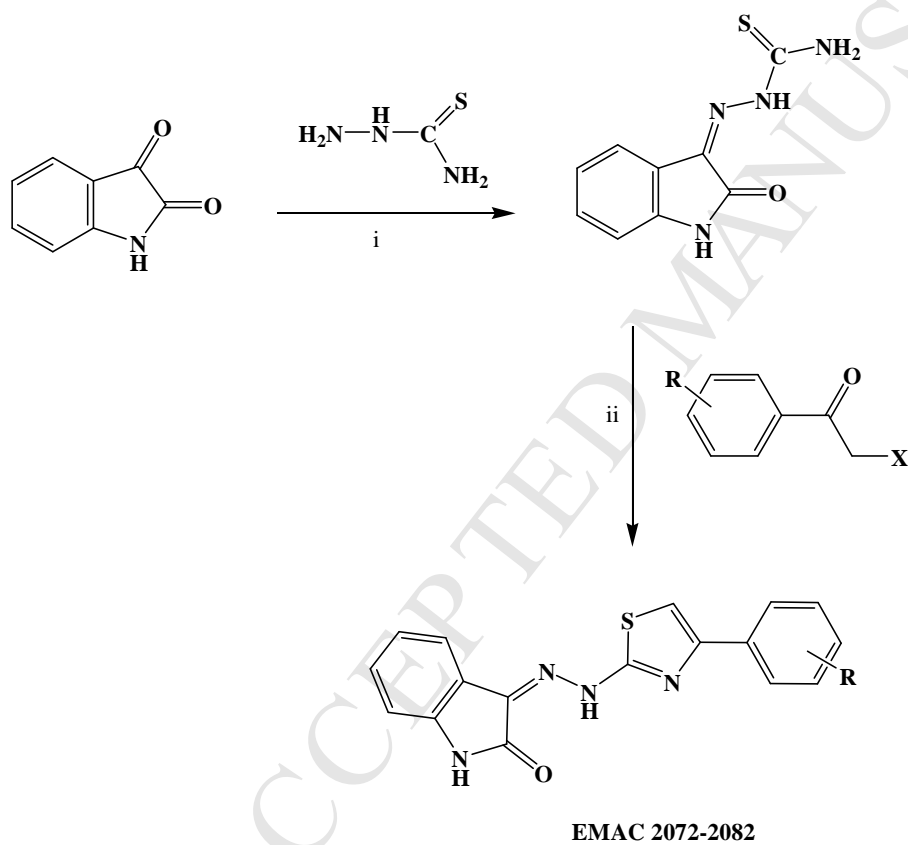
<sup>a</sup>Compound concentration required to reduce the HIV-1 RT-associated RNase H activity by 50%

<sup>b</sup>Compound concentration required to reduce the HIV-1 RT-associated RNA-dependent DNA polymerase activity by 50%. <sup>c</sup>ND, not done.

Figure 1

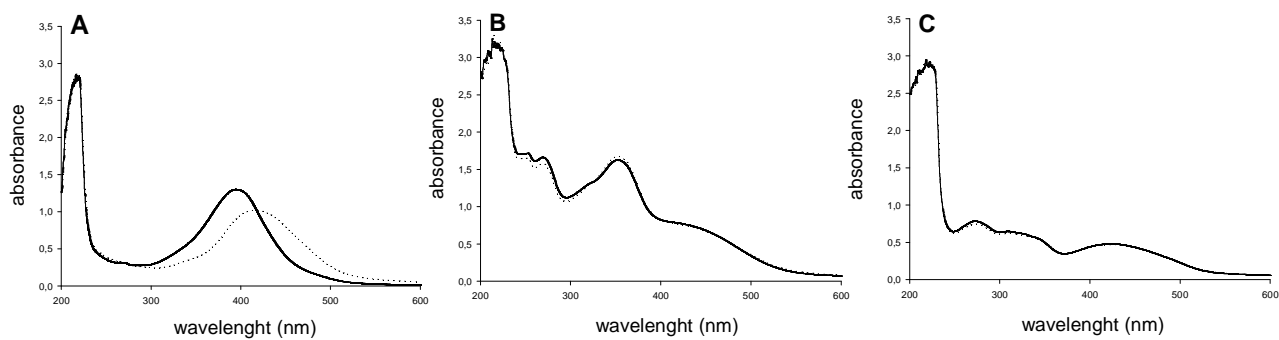


Scheme 1



R: 4-Cl, 4-F, 4-Br, 4-NO<sub>2</sub>, 4-C<sub>6</sub>H<sub>5</sub>, 2,4-F, 3-NO<sub>2</sub>, 4-CH<sub>3</sub>, 4-OCH<sub>3</sub>, H, 2,4-Cl  
 X: Cl or Br

Figure 2



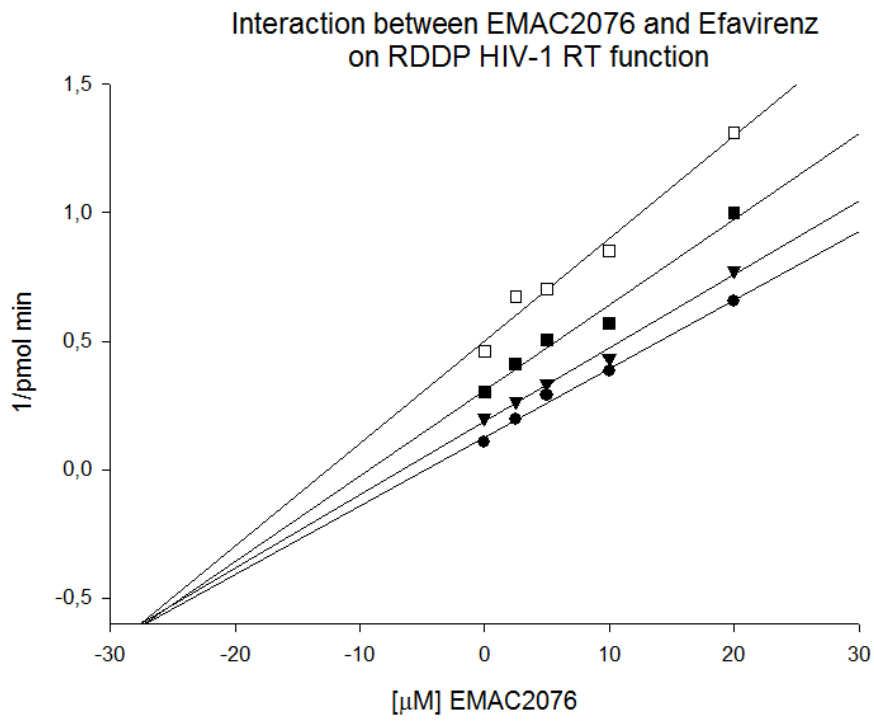
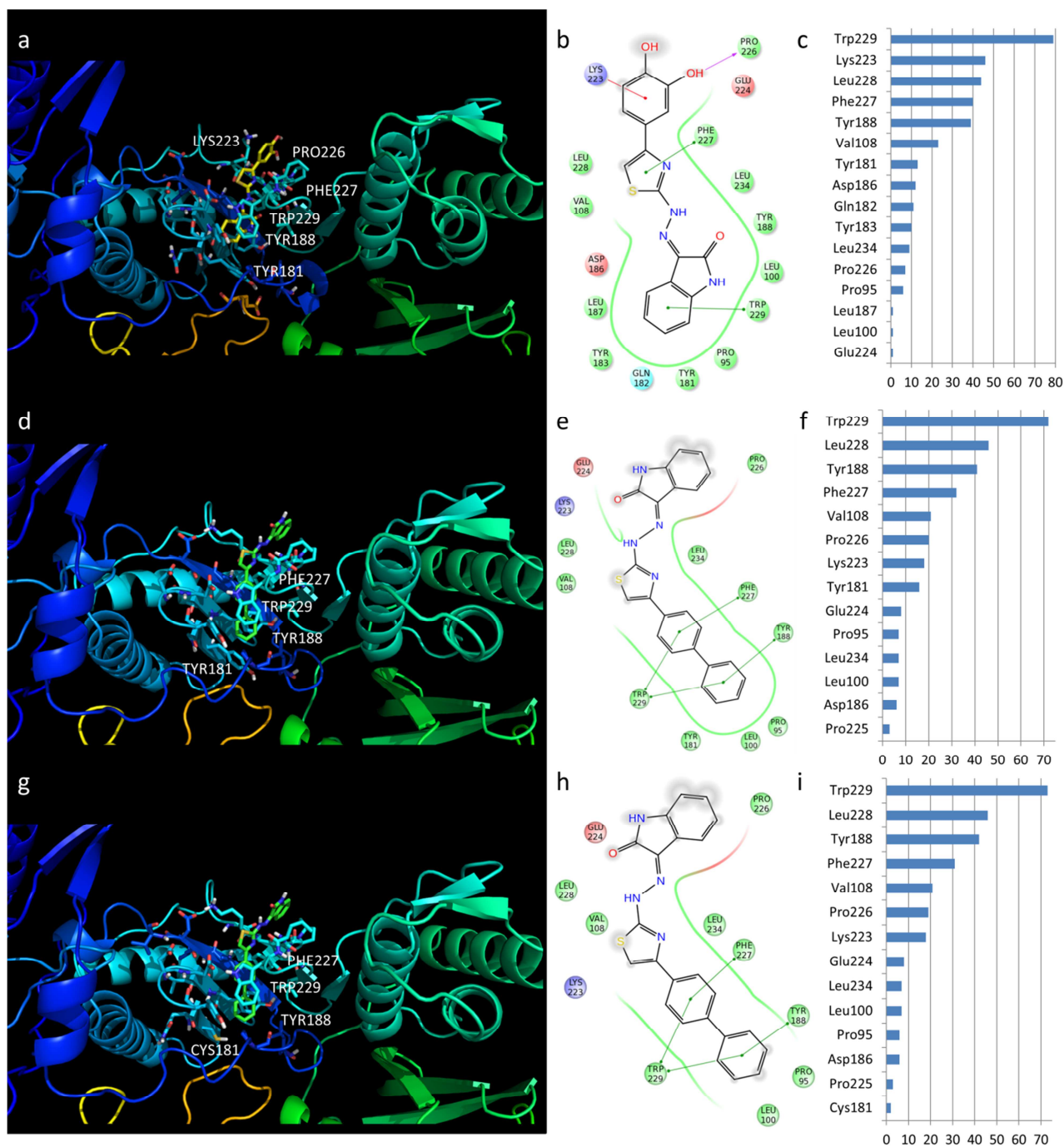
**Figure 3**

Figure 4



**Highlights**

- A series of indolinones derivatives has been synthesized and characterised.
- The compounds showed to be HIV 1 RT dual inhibitors in the low micromolar range.
- A protocol to investigate the mode of action has been devised.
- Compounds do not bind  $Mg^{++}$  ions in the RNase H catalytic site.
- Activity is not affected by common NNRTIBP RT mutations.

## SUPPLEMENTARY DATA

**(Z)-3-(2-(4-arylthiazol-2-yl)hydrazono)indolin-2-one Derivatives as Dual Inhibitors of HIV-1 Reverse Transcriptase**

Rita Meleddu, Simona Distinto, Angela Corona, Giulia Bianco, Valeria Cannas, Francesca Esposito, Anna Artese, Stefano Alcaro, Peter Matyus, Dora Bogdand, Filippo Cottiglia, Enzo Tramontano, Elias Maccioni.

**Table of Contents**

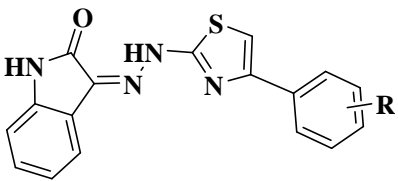
**Table S1.** Chemical and physical data of derivatives **EMAC2072-2082**

**Table S2.** Analytical data of derivatives **EMAC2072-2082**

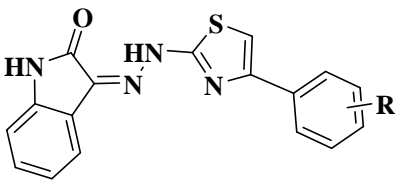
**Figure S1.** NOE effect for *E* and *Z* configuration.

**Table S3:** Docking scores, post-docking energies and main active site residues interactions.

**Figures S2-** NMR spectra.

**Table S1.** Chemical-physical and spectroscopic properties of derivatives **EMAC2072-2082**


Compound	R	Mp (C°)	% Yield	CHN% Calc (Found)	m/z
<b>EMAC2072</b>	4-Cl	>250	73	57.55 (57.34); 3.12 (3.13); 15.79 (15.85)	354; 356; 326; 328; 210; 212; 146
<b>EMAC2073</b>	4-F	>250	57	60.34 (60.10); 3.28 (3.27); 16.56 (16.62)	338; 310; 194; 146
<b>EMAC2074</b>	4-Br	>250	95	51.14 (50.98); 2.78 (2.77); 14.03 (13.98)	400; 398; 372; 370; 256; 254; 146
<b>EMAC2075</b>	4-NO <sub>2</sub>	>250	84	55.88 (56.06); 3.03 (3.04); 19.17 (19.10)	365; 337; 221; 146
<b>EMAC2076</b>	4-C <sub>6</sub> H <sub>5</sub>	>250	96	69.68 (69.46); 4.07 (4.08); 14.13 (14.18)	396; 368; 252; 146
<b>EMAC2077</b>	2,4-F	>250	66	57.30 (57.12); 2.83 (2.82); 15.72 (15.67)	356; 328; 212; 146
<b>EMAC2078</b>	3-NO <sub>2</sub>	>250	86	55.88 (56.05); 3.03 (3.02); 19.17 (19.24)	365; 337; 221; 146
<b>EMAC2079</b>	4-CH <sub>3</sub>	>250	72	64.65 (64.43); 4.22 (4.21); 16.75 (16.81)	334; 306; 190; 146
<b>EMAC2080</b>	4-OCH <sub>3</sub>	>250	84	61.70 (61.48); 4.03 (4.04); 15.99 (15.94)	350; 322; 206; 146
<b>EMAC2081</b>	H	250	92	63.73 (63.95); 3.78 (3.79); 17.49 (17.56)	320; 292; 176; 146
<b>EMAC2082</b>	2,4-Cl	>250	90	52.45 (52.62); 2.59 (2.60); 14.39 (14.44)	388; 390; 360; 362; 244; 246; 146

**Table S2.** Analytical data of derivatives **EMAC2072-2082**


Compound	R	Reaction solvent	Crystallisation solvent	Aspect	Reaction time (h)
<b>EMAC2072</b>	4-Cl	2-propanol	Water/Ethanol	Yellow-orange solid	24
<b>EMAC2073</b>	4-F	2-propanol	Water/Ethanol	Yellow-orange solid	12
<b>EMAC2074</b>	4-Br	2-propanol	Water/Ethanol	Yellow-orange solid	24
<b>EMAC2075</b>	4-NO <sub>2</sub>	2-propanol	Water/Ethanol	Yellow-orange solid	24
<b>EMAC2076</b>	4-C <sub>6</sub> H <sub>5</sub>	2-propanol	Water/Ethanol	Yellow-orange solid	12
<b>EMAC2077</b>	2,4-F	2-propanol	Water/Ethanol	Yellow-orange solid	24
<b>EMAC2078</b>	3-NO <sub>2</sub>	2-propanol	Water/Ethanol	Yellow-orange solid	12
<b>EMAC2079</b>	4-CH <sub>3</sub>	2-propanol	Water/Ethanol	Yellow-orange solid	12
<b>EMAC2080</b>	4-OCH <sub>3</sub>	2-propanol	Water/Ethanol	Yellow-orange solid	24
<b>EMAC2081</b>	H	2-propanol	Water/Ethanol	Yellow-orange solid	12
<b>EMAC2082</b>	2,4-Cl	2-propanol	Water/Ethanol	Yellow-orange solid	12

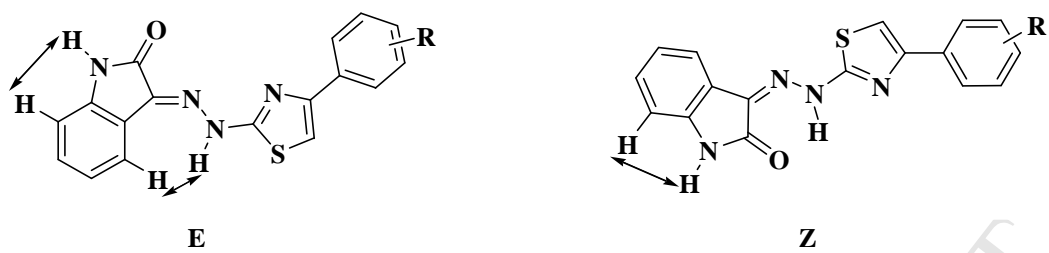
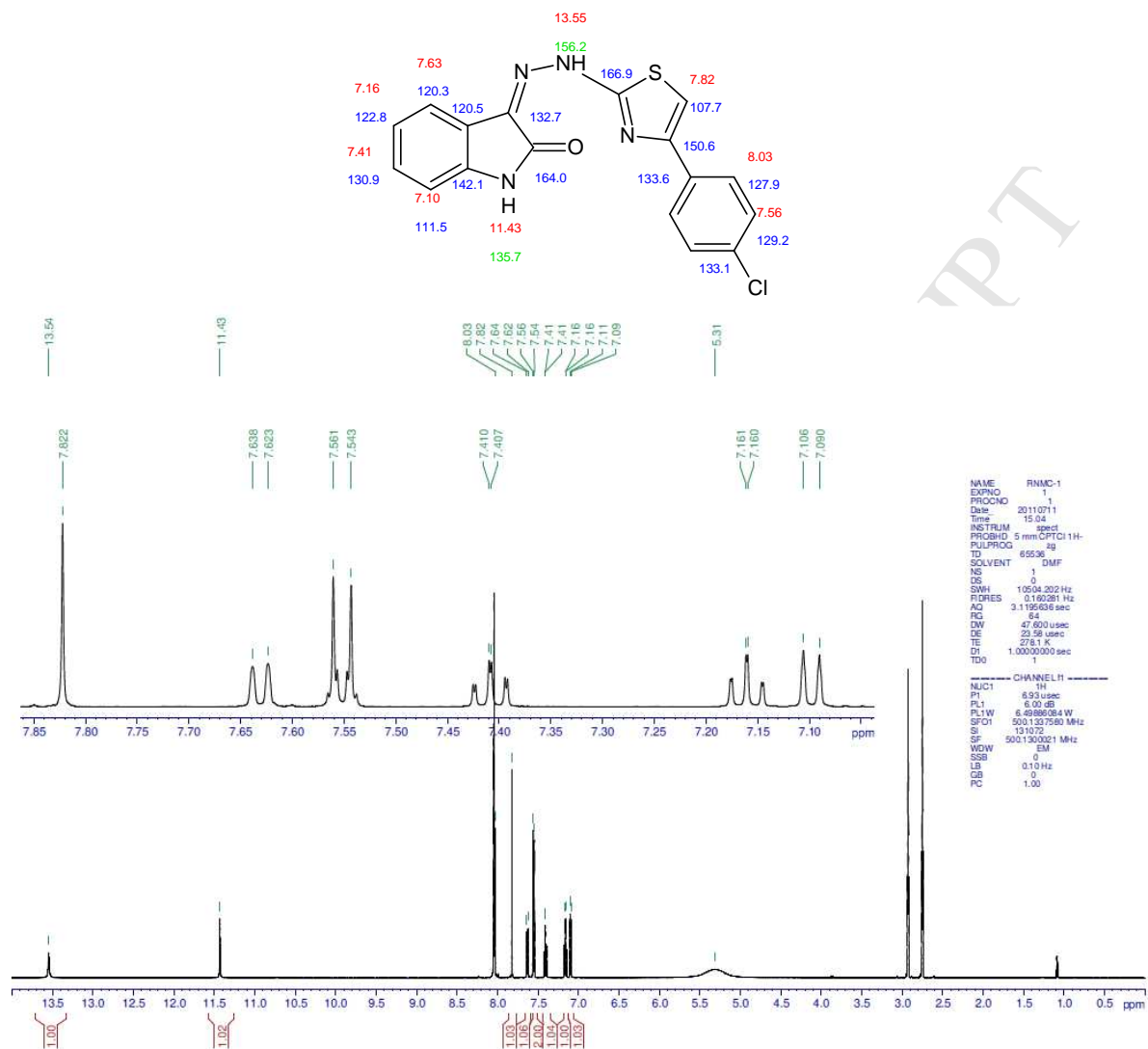


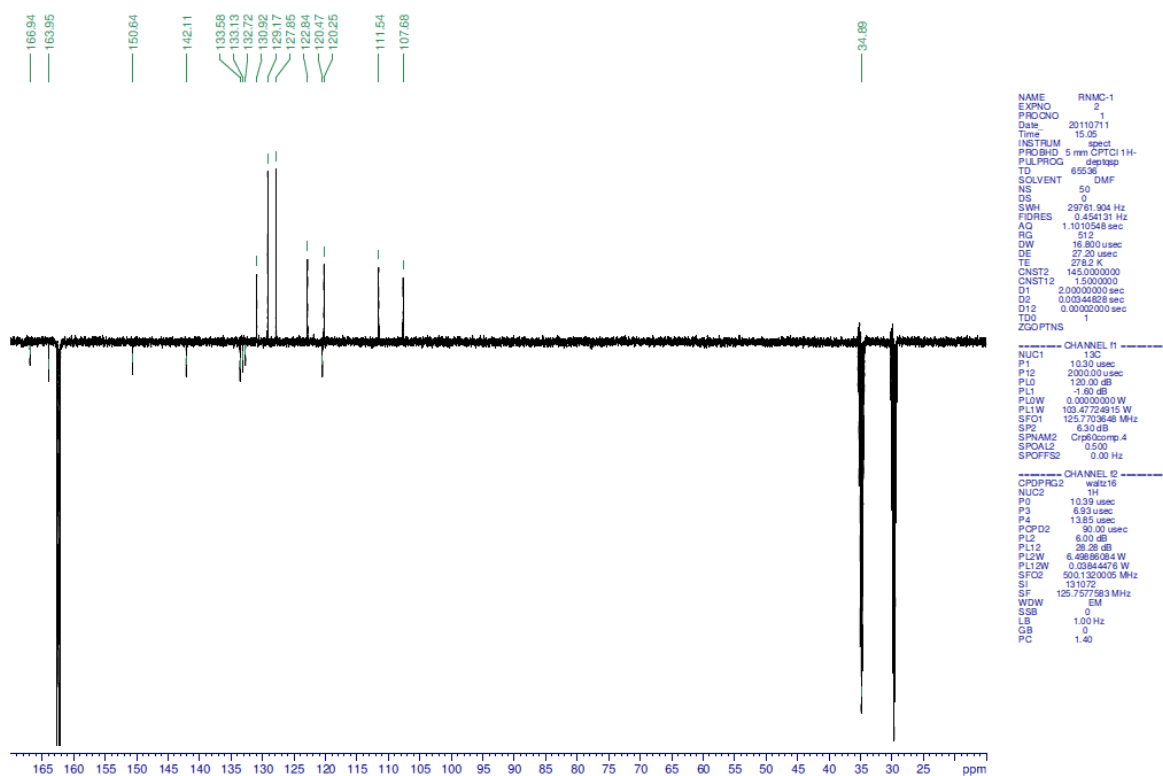
**Figure S1.** NOE effect for *E* and *Z* configuration.

**Table S3:** Docking scores, post-docking energies and main active site residues interactions.

Complex	Glide GScore	$\Delta G$ -bind (Kcal* $\text{mol}^{-1}$ )	Active site residues interaction			
			HBond	Distance D---A ( $\text{\AA}$ )	$\pi$ - $\pi$ and cation- $\pi$	Distance (between aromatic centroids) ( $\text{\AA}$ )
Compound 1-RT	-7.3	-49.46	OH--- O(Pro226)	2.7	Thiaz--- Phe227, Indol--- Trp229, Phe--- Lys223	5 (edge to face) 3.47 (face to face) 3.28 (cation - $\pi$ )
EMAC2076-RT	-8.13	-43.87			Phe1--- Phe227, Phe2--- Tyr188; Phe1--- Trp229; Phe--- Trp229	5.1 (edge to face) 4.13 (parallel) 4 (parallel); 4.2 (parallel)
EMAC2076- Y181CRT	-7.89	-42.89			Phe1--- Phe227, Phe2--- Tyr188; Phe1--- Trp229; Phe--- Trp229	5.15 (edge to face) 4.06 (parallel) 4.2 (parallel); 4.2 (parallel)

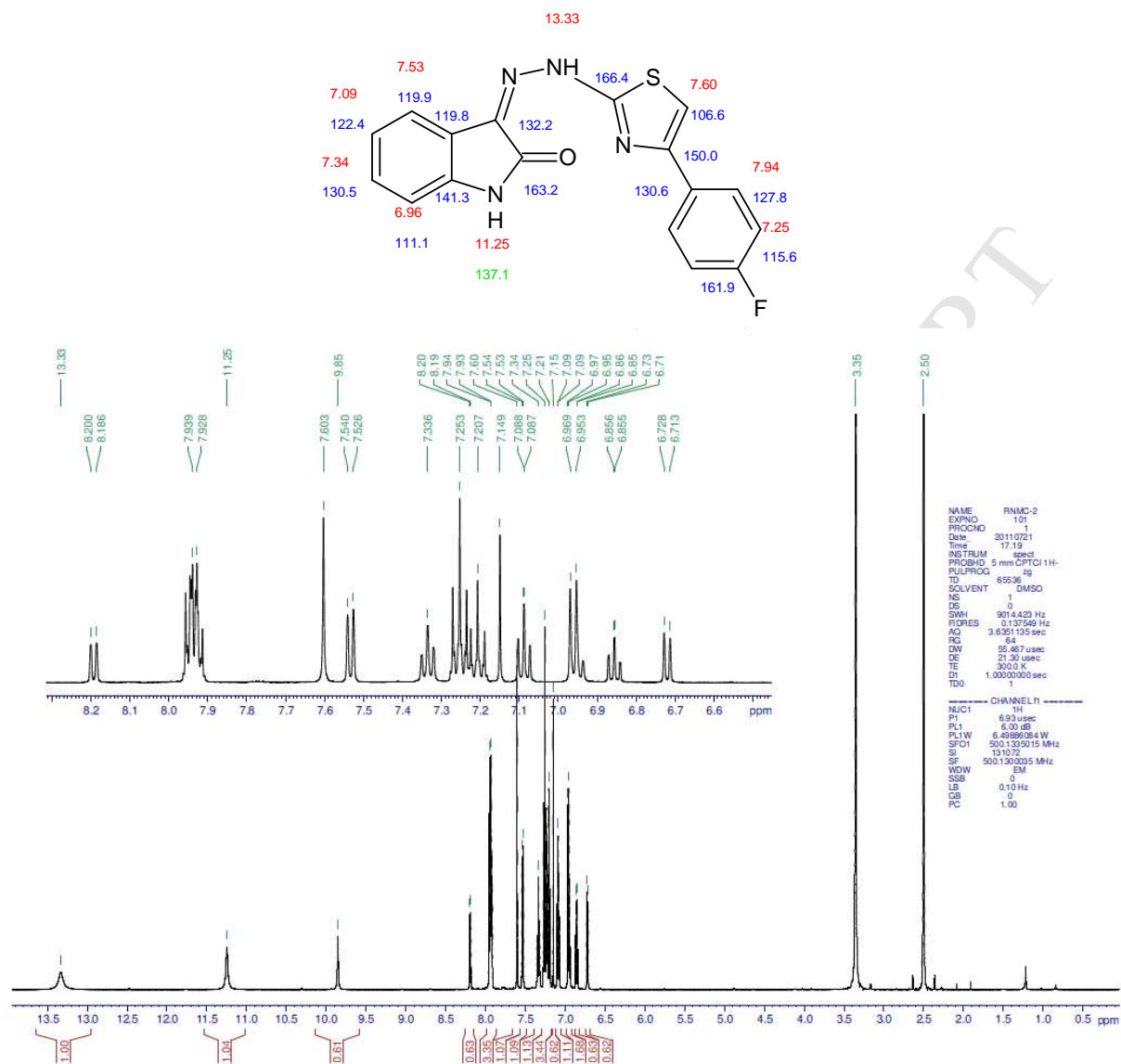
Figures S2 NMR spectra:  $^1\text{H}$ , with enlargement of the aromatic part, and DEPTQ  $^{13}\text{C}$  of new synthesized compounds:  
EMAC2072





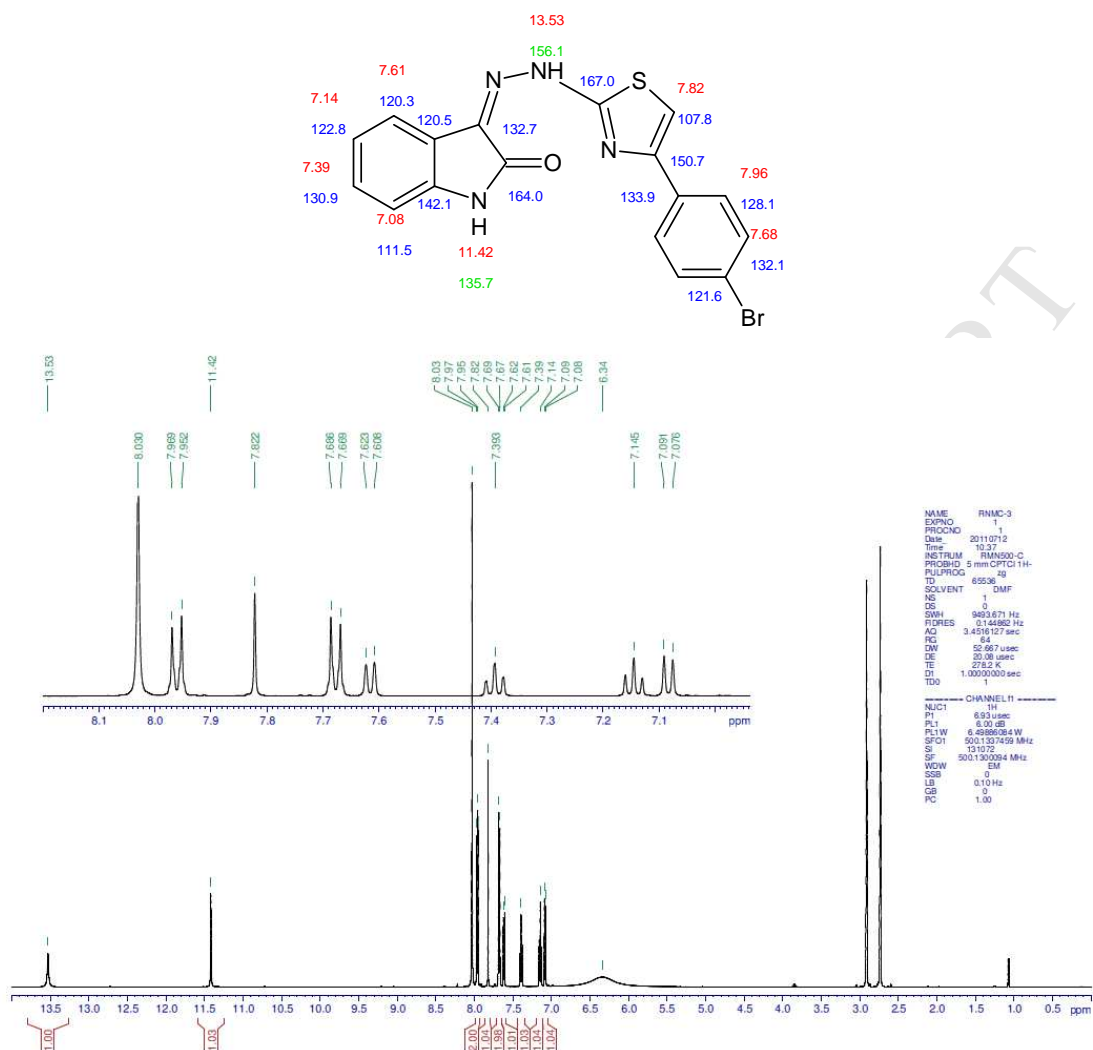
ACCEPTED MANUSCRIPT

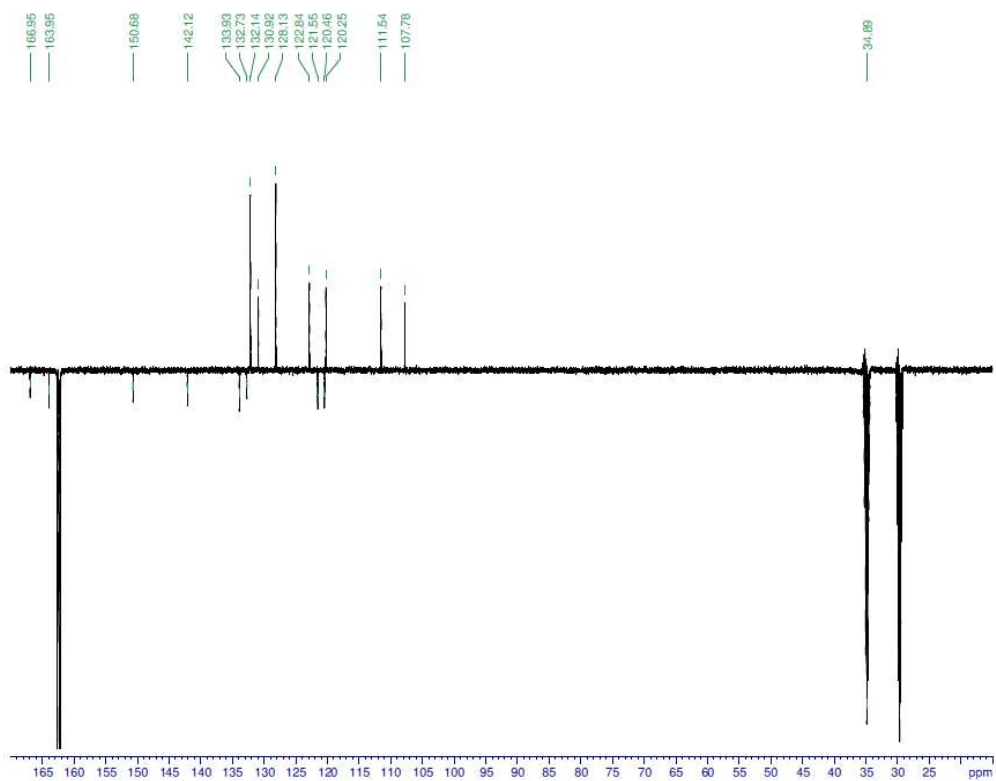
EMAC2073





EMAC2074





```

NAME      RNM-3
EXPNO     2
PROCNO    2
Date_     20110712
Time      10.44
INSTRUM   spect
PROBHD    5 mm CPTCI 1H-
PULPROG   zgpg30
TD         65536
SOLVENT   DMF
NS         144
DS         0
SWH        23701.304 Hz
FIDRES     0.454131 Hz
AQ         1.1010548 sec
RG         312
DW         16.800 usec
DE         27.30 usec
TE         278.2 K
CNST1     145.000000
CNST12    1.5000000
D1         2.0000000 sec
D2         0.0004468 sec
D12        0.0002000 sec
TD0        1
ZGPGTNS    1

```

```

----- CHANNEL f1 -----
NUC1       13C
P1         10.30 usec
P12        2000.00 usec
PL0        120.00 dB
PL1        -1.00 dB
PL1W       0.0000000 W
PL1W       103.47724915 W
SFO1       125.7703648 MHz
SFO2       6.300 MHz
SFO3        Crp60comp.4
SFOAL3     0.500
SFOFFS2    0.00 Hz

```

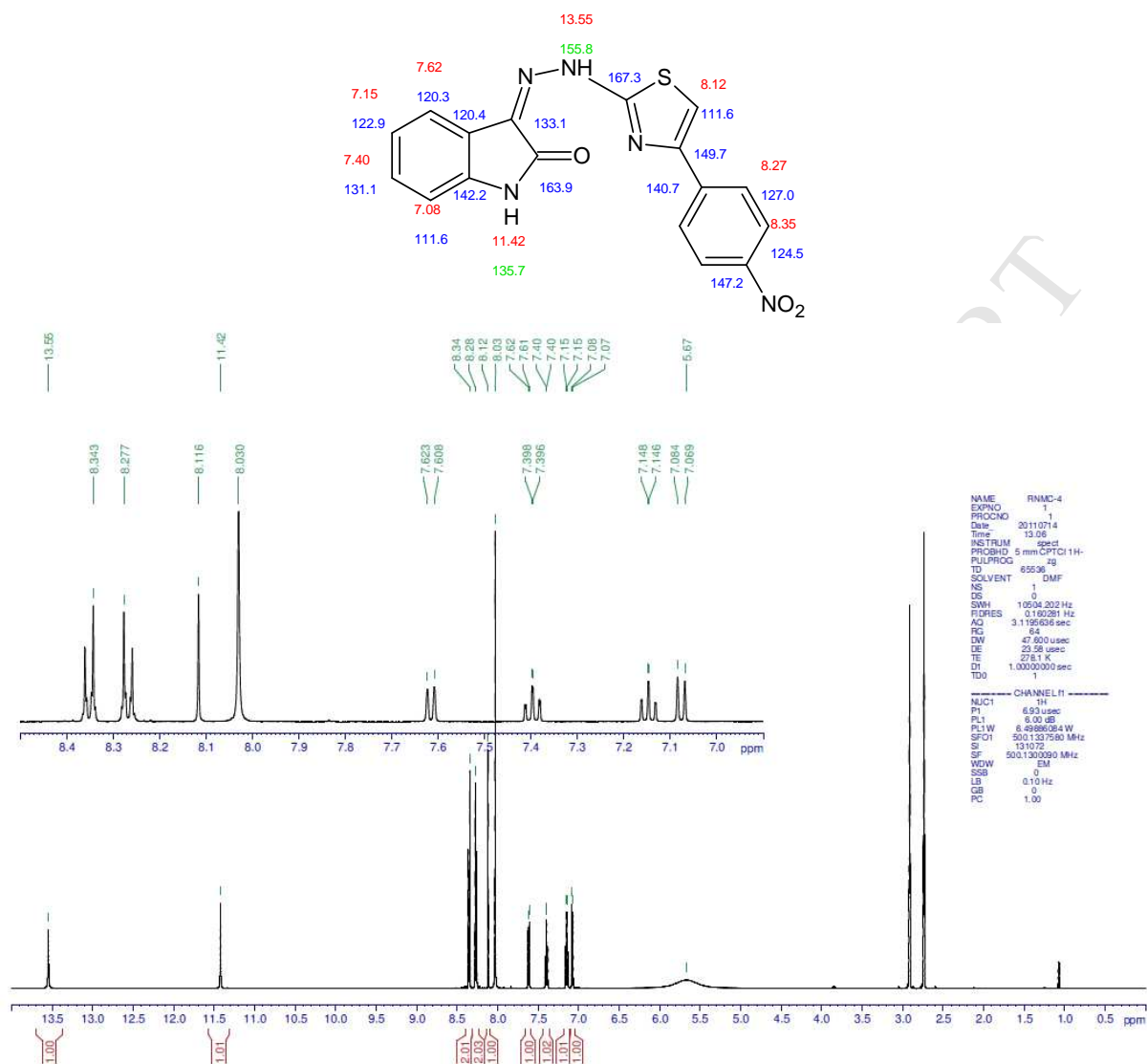
```

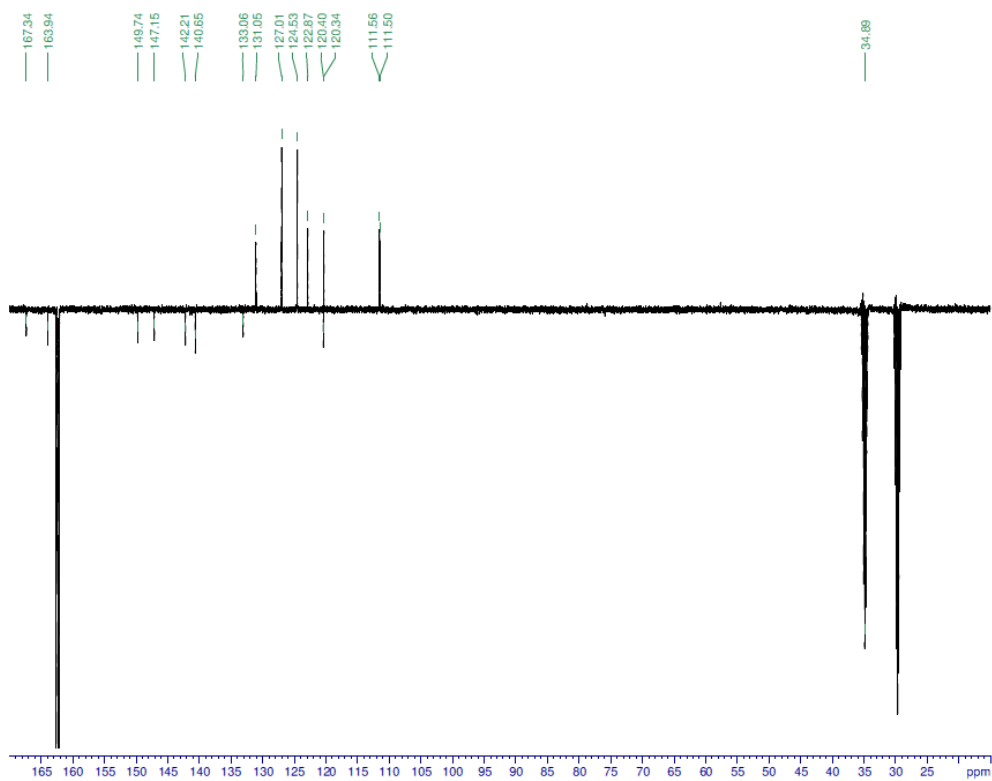
----- CHANNEL f2 -----
CPDPRG2   waltz16
NUC2       1H
P0         10.39 usec
P3         6.93 usec
P4         13.85 usec
PCPD2     50.00 usec
PL2        6.93 dB
PL12       28.28 dB
PL12W     6.62896304 W
PL12W     0.03844478 W
SFO2       500.1363005 MHz
SI         131072
SF         125.7577584 MHz
WDW        EM
SSB        0
LS         1.00 Hz
GB         0
PC         1.40

```

ACCEPTED MANUSCRIPT

EMAC2075



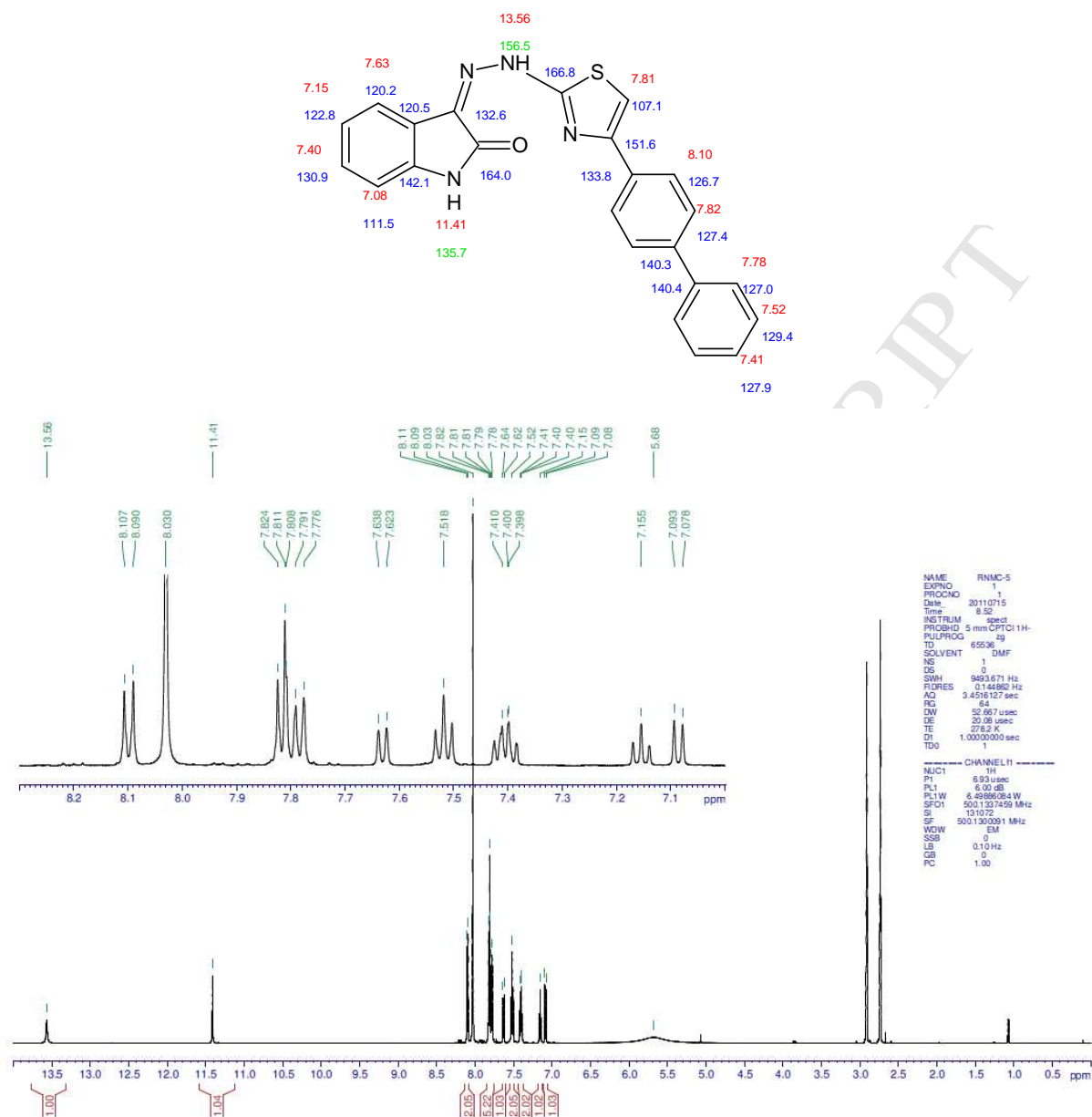


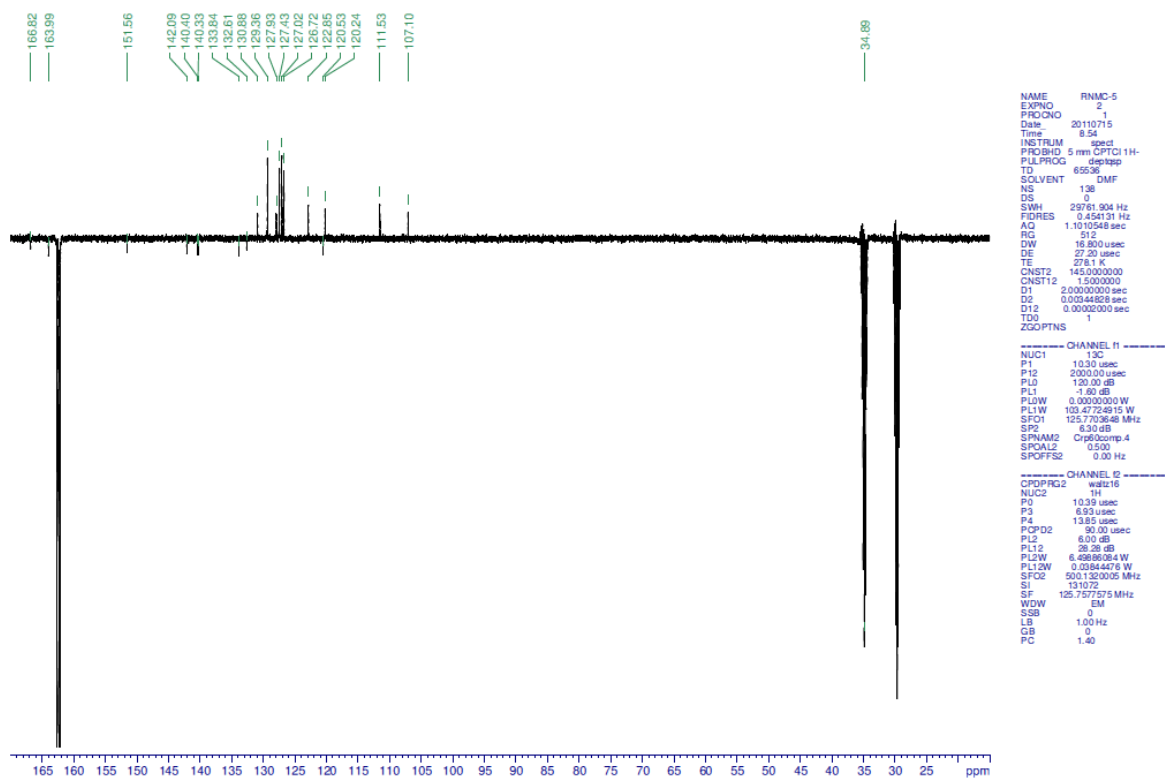
```
NAME RMMC-4
EXPNO 2
PROCNO 1
Date_ 20110714
Time 13.18
INSTRUM spect
PROBHD 5mm CPTCI 1H-
PULPROG zgpg30
TD 65536
SOLVENT DMF
NS 88
DS 0
SWH 29761.934 Hz
FIDRES 0.454151 Hz
AQ 1.1010548 sec
RG 512
DW 16.800 usec
DE 27.20 usec
TE 278.1 K
CONST1 145.000000
CONST12 1.500000
D1 2.00000000 sec
D2 0.00344805 sec
D12 0.00050000 sec
TD0 ZGPGTNS
1
```

```
----- CHANNEL f1 -----
NUC1 13C
P1 10.00 usec
P2 2000.00 usec
PL0 120.00 dB
PL1 -1.60 dB
PL0W 0.00000000 W
PL1W 100.47204915 W
SFO1 125.770846 MHz
SP 6.00 dB
SFO2 500.1320005 MHz
SFOAL2 0.500
SFOAL3 0.00 Hz
```

```
----- CHANNEL G2 -----
CPDPRG2 waltz16
NUC2 1H
P0 10.00 usec
P3 6.93 usec
P4 13.85 usec
PCPD2 90.00 usec
PL2 6.00 dB
PL3 28.28 dB
PL2W 6.45886084 W
PL3W 0.00844476 W
SFO2 500.1320005 MHz
SI 131072
SF 125.7577581 MHz
WDW EM
SSB 0
LB 1.00 Hz
GB 0
PC 1.40
```

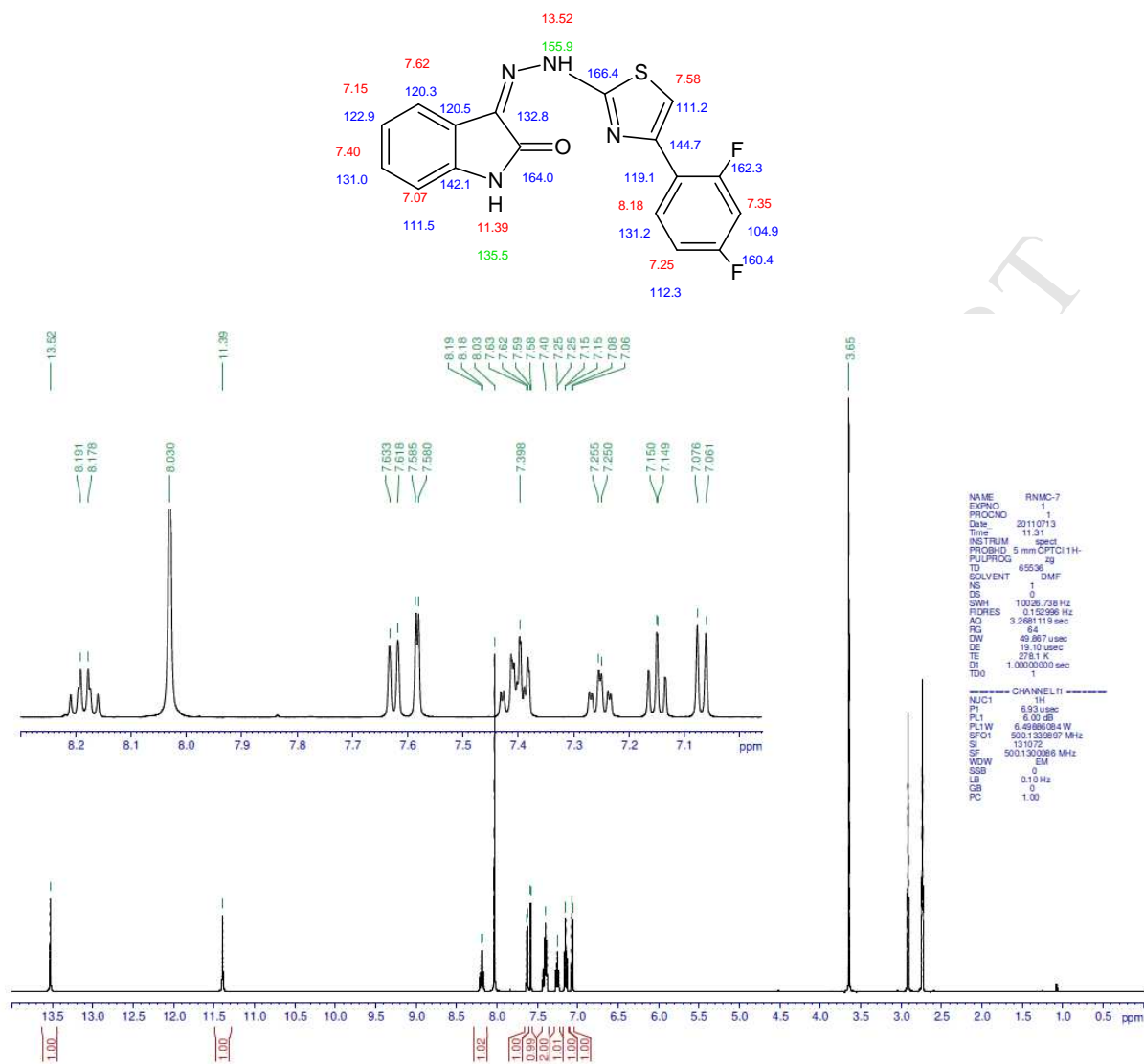
EMAC2076

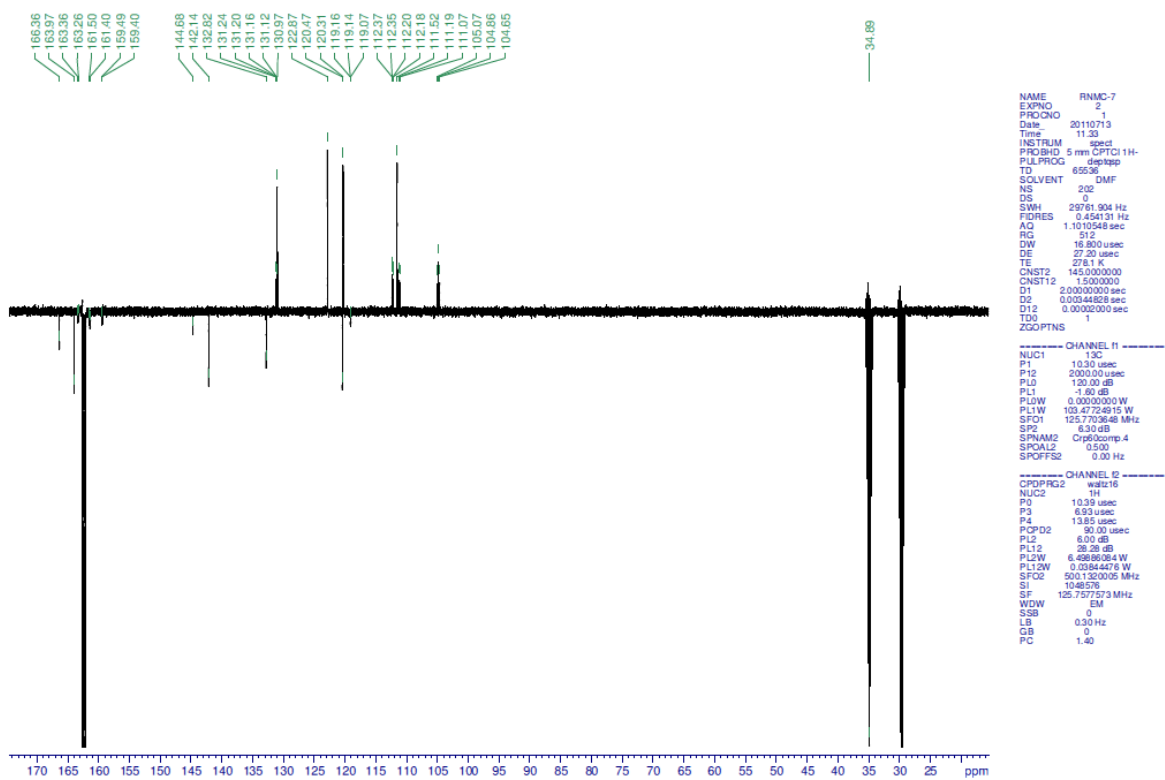




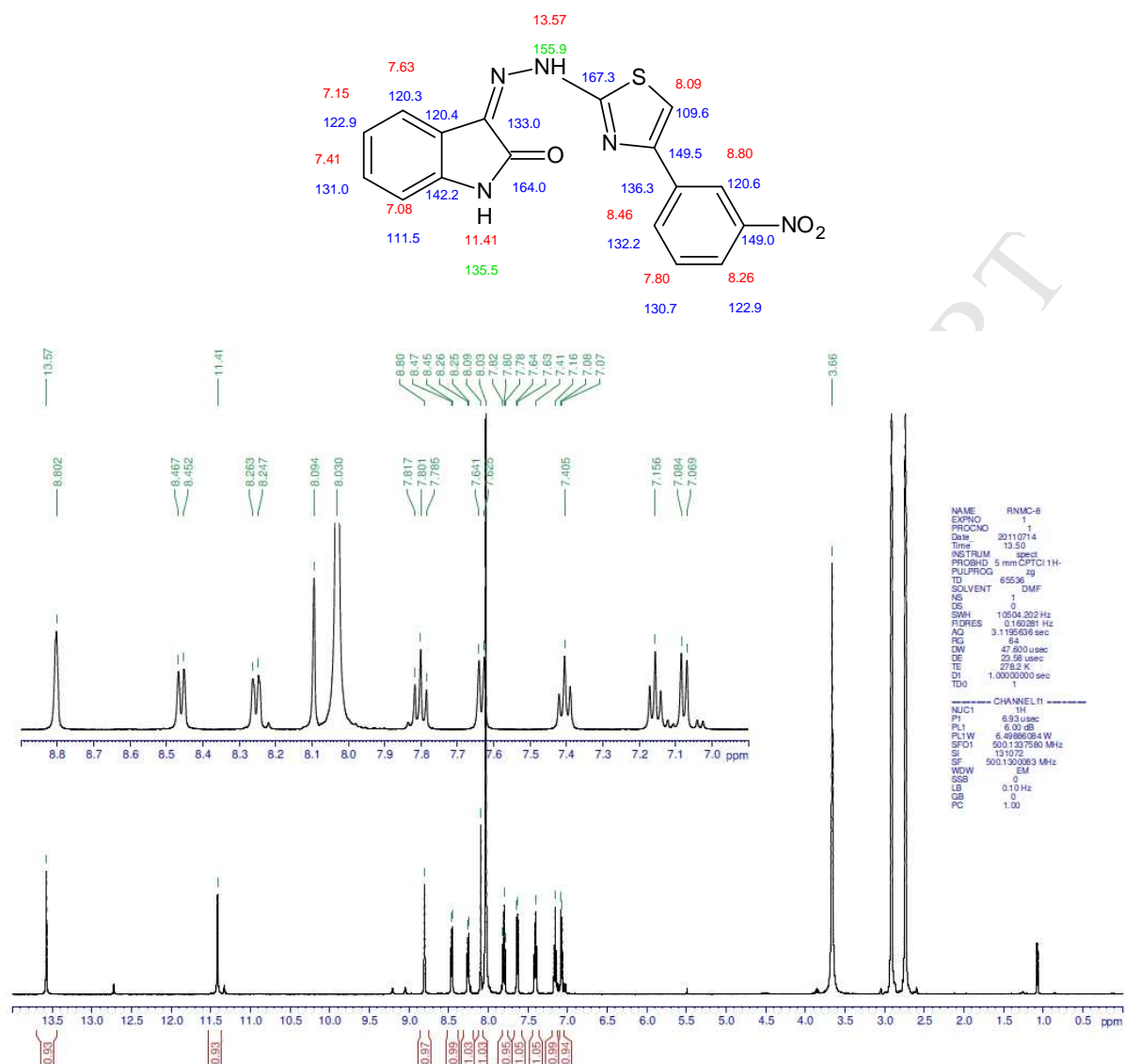
ACCEPTED MA

EMAC2077



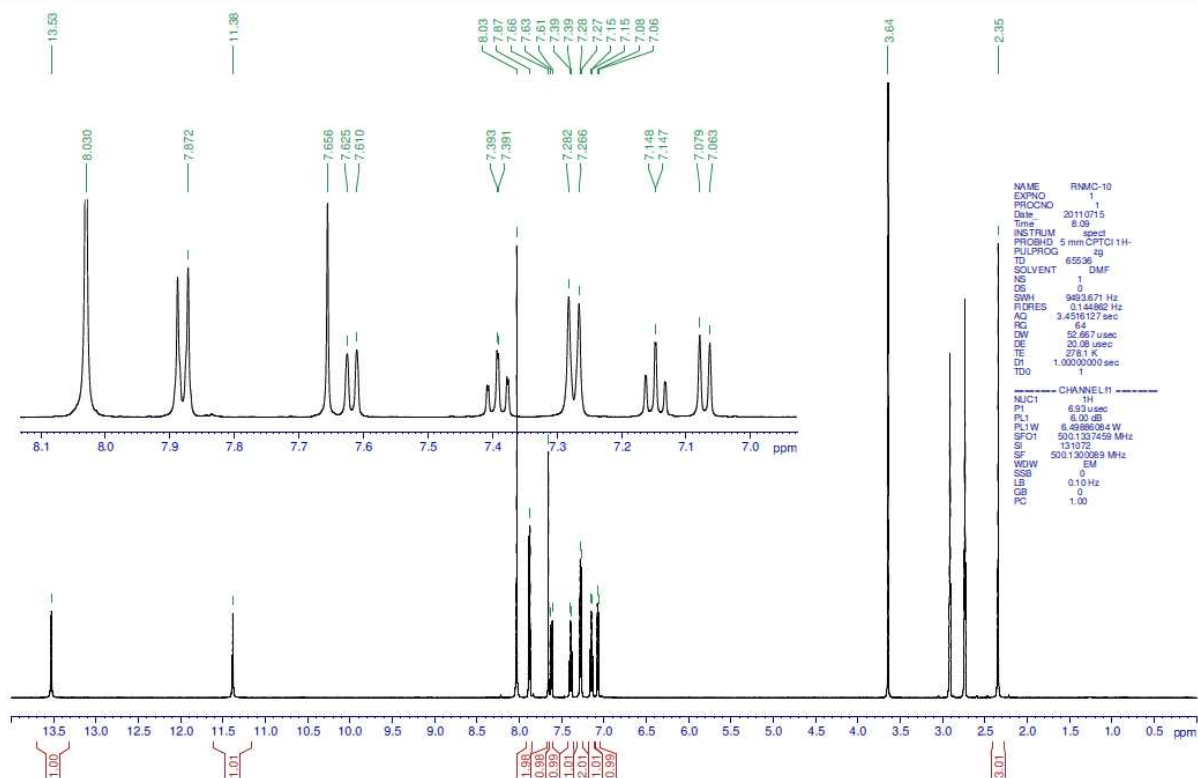
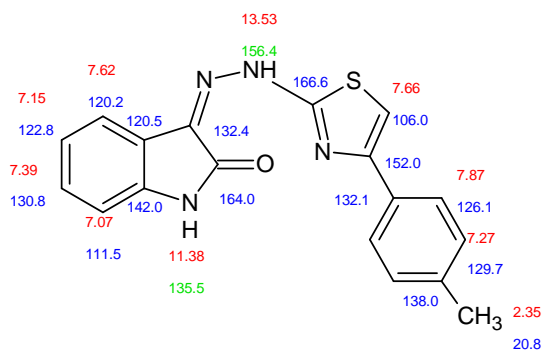


EMAC2078



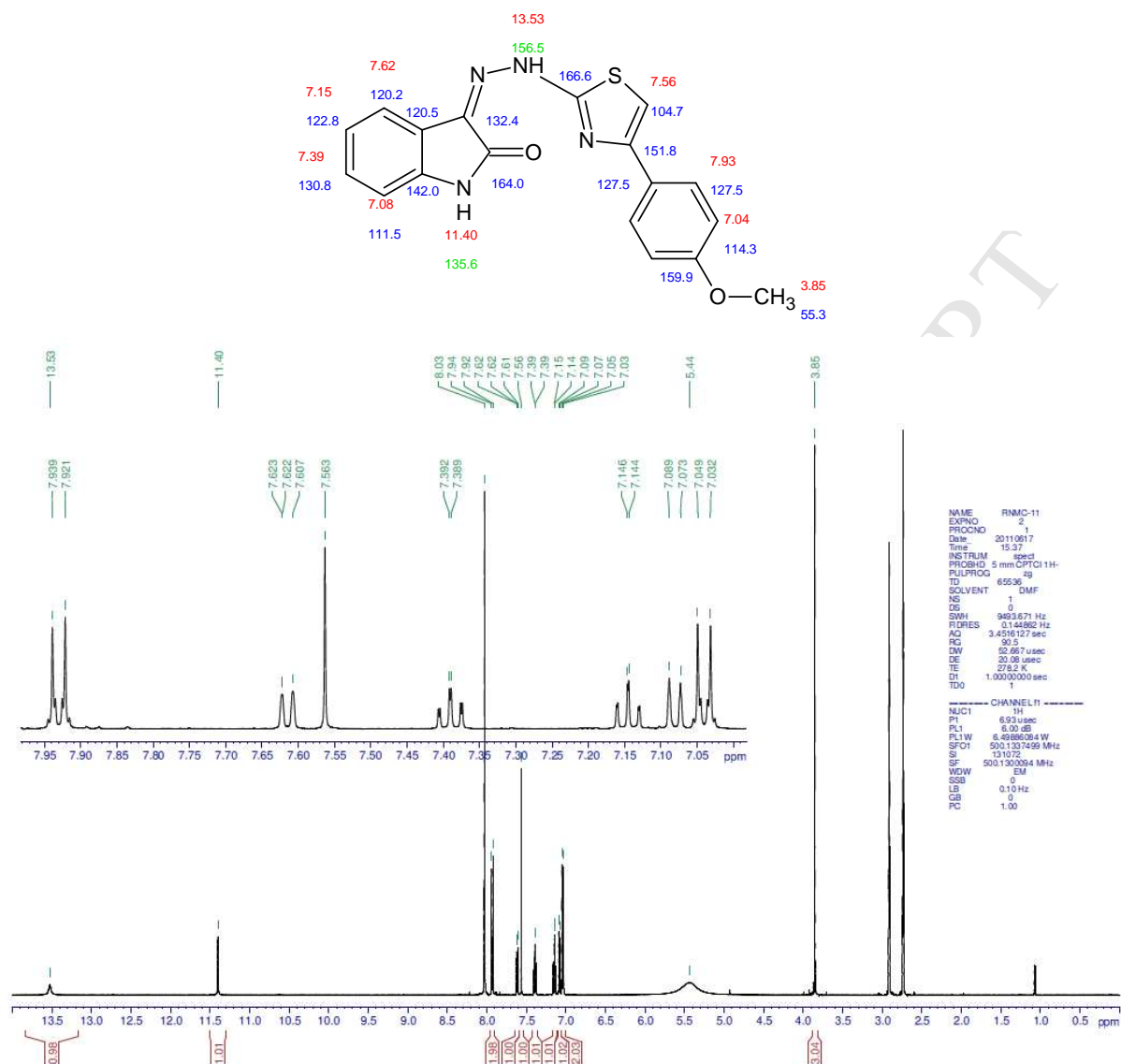


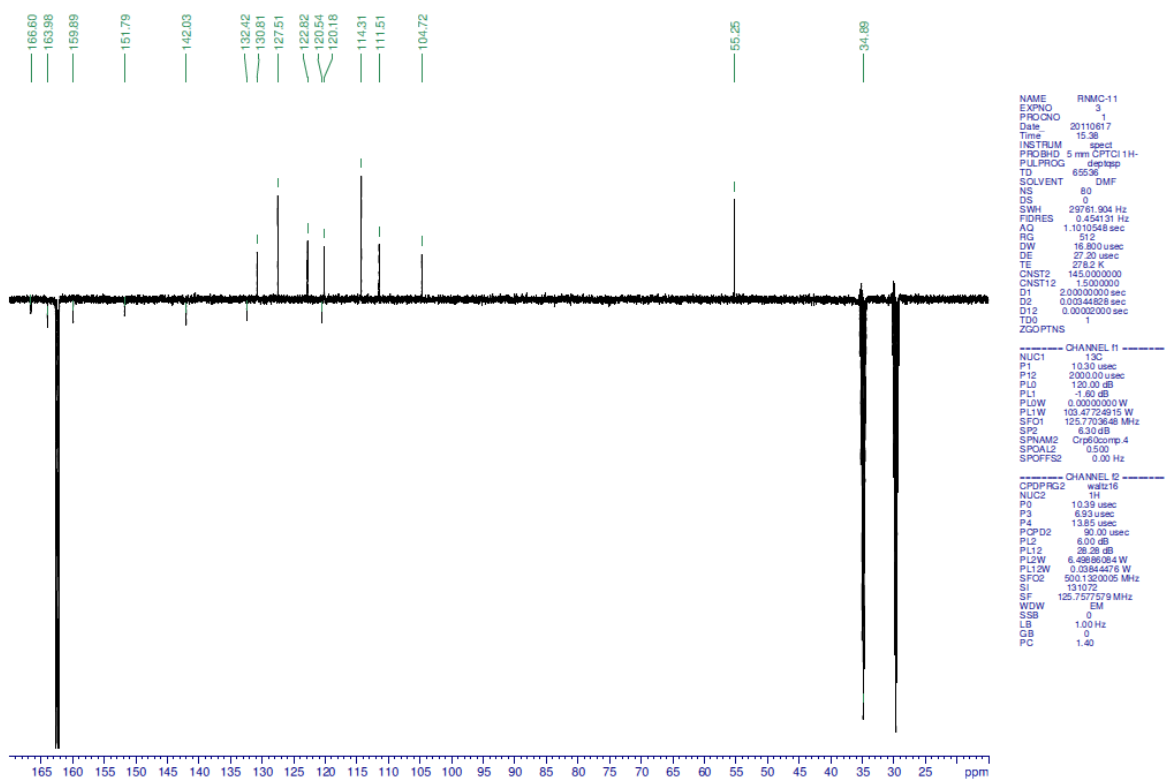
EMAC2079





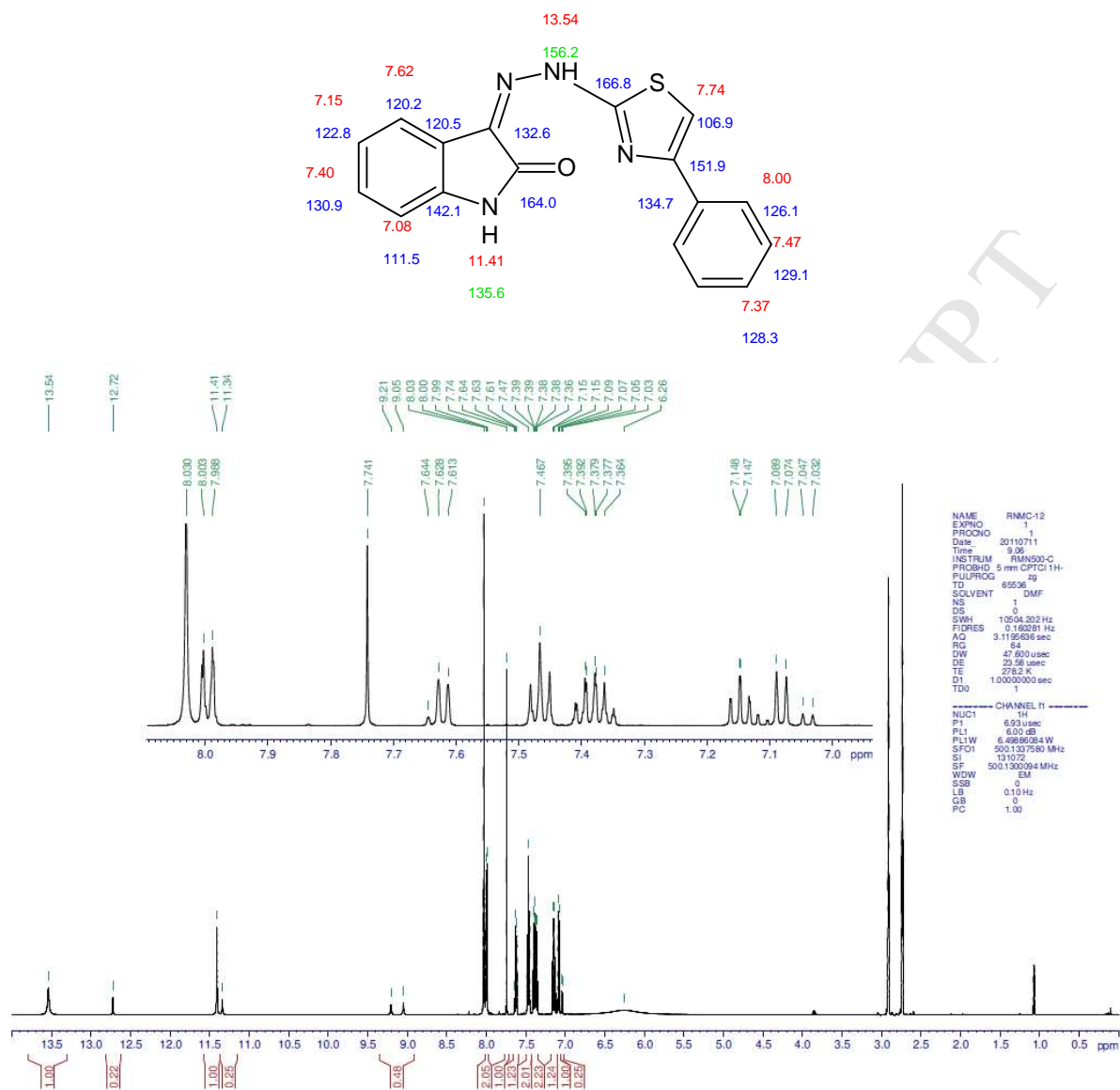
EMAC2080





ACCEPTED MANUSCRIPT

EMAC2081





EMAC2082

